SOT FGによる物理量診断

Solar-B国内会議　2005.10.31　　一本　潔

SOT 4 つの観測パス

	NFI	BFI	SP	CT
pixel scale (arcsec/pix)	**0.08**	**0.054**	**0.16**	**0.22**
maximum FOV (arcsec^2) (EWxNS)	**328x164**	**218x109**	**328 (scan range) x164 (slit length)**	**11x11**
wavelength resolution (A)	**~0.1**	**3~10**	**0.02**	**5**
number of wavelength in a data set	**1~4**	**1**	**244**	**1**
time resolution (typical)	**10~30s**	**1~10s**	**~1hr**	**580Hz**
photometric accuracy (%)	**0.1 ~ 0.5**	**0.5**	**< 0.1**	**~0.5**

NFI: Narrowband Filtergraph Instrument
BFI: Broadband Filtergraph Instrument
SP: Spectro-Polarimeter
CT: Correlation Tracker

SOT performance

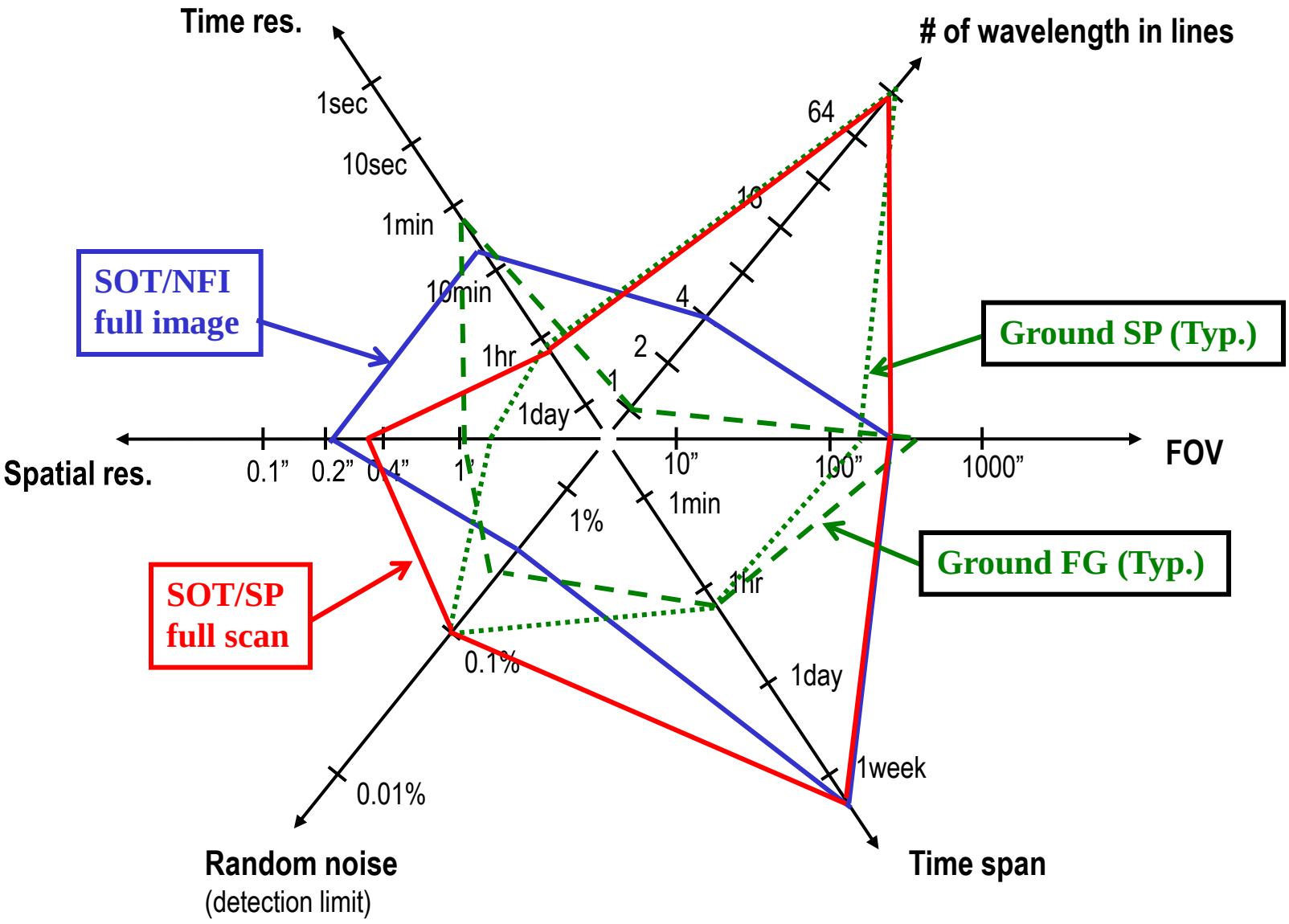

SOT 観測波長

Ion	λ , Å	Purpose	g_{eff}	BFI	NFI	SP	CT
CN I	3883.0	Magnetic Network Imaging	-	✓			
Ca II H	3968.5	Chromospheric Heating	1.33	✓			
CH I	4305.0	Magnetic Elements	-	✓			
	4504.5	Blue Continuum		✓			
Mg I b	5172.7	Chromospheric Dopp./ Mag.	1.75		✓		
Fe I	5247.1	Photospheric Magnetograms	2.00		✓		
Fe I	5250.2	Photospheric Magnetograms	3.00		✓		
Fe I	5250.6	Photospheric Magnetograms	1.50		✓		
	5550.5	Green Continuum		✓			
Fe I	5576.1	Photospheric Dopplergrams	0.00		✓		
Na I	5895.9	Chromospheric Dopp/Mag.	1.33		✓		
Fe I	6301.5	Photospheric Magnetograms	1.67		✓	✓	
Fe I	6302.5	Photospheric Magnetograms	2.50		✓	✓	
Ti I	6303.8	Umbral Magnetograms	0.92		✓		
	6320.0	Broadband WL for CT	-				✓
H I	6562.8	Chromospheric Structure	1.33		✓		
	6684.0	Red Continuum		✓			

BFI

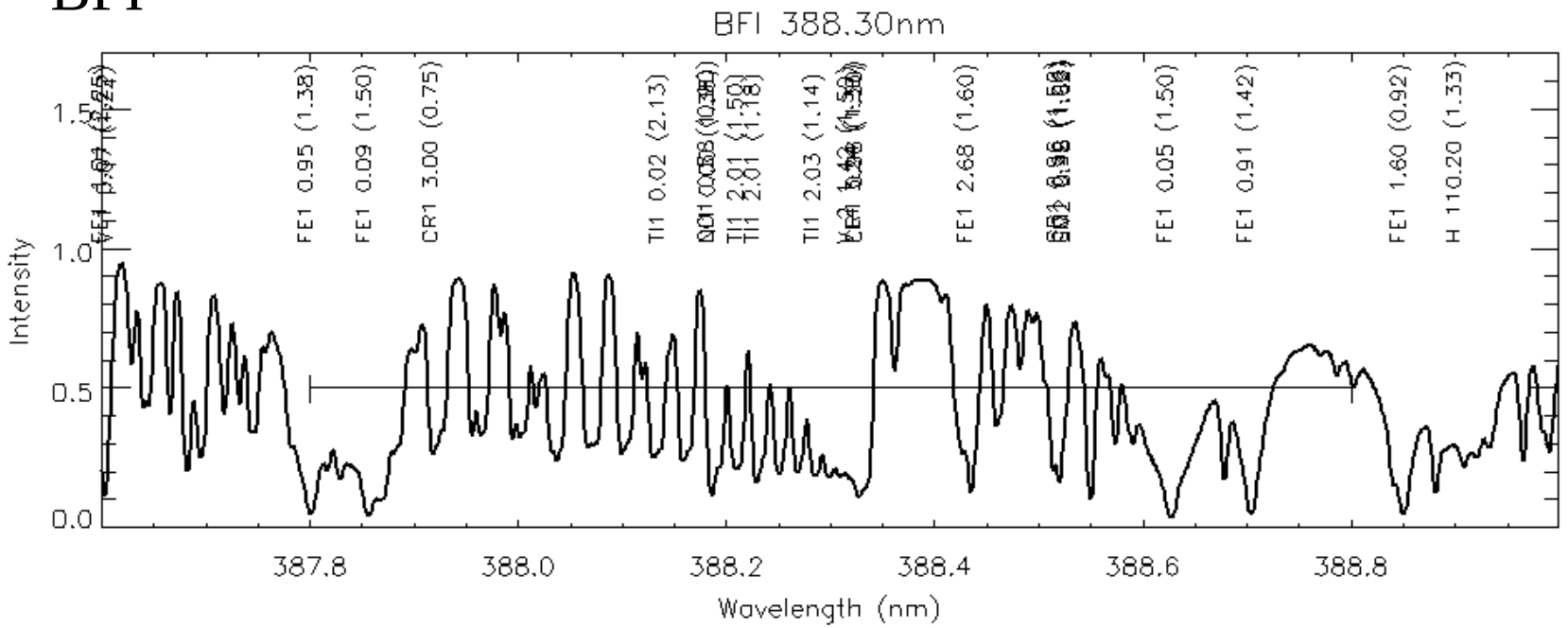
BFI 388.30nm
FE1 0.95 (1.38)
FE1 0.09 (1.50)
CR1 3.00 (0.75)
TI1 0.02 (2.13)
TI1 2.03 (1.14)
FE1 2.68 (1.60)
FE1 0.05 (1.50)
FE1 0.91 (1.42)
FE1 1.60 (0.92)
H 110.20 (1.33)
Intensity
Wavelength (nm)

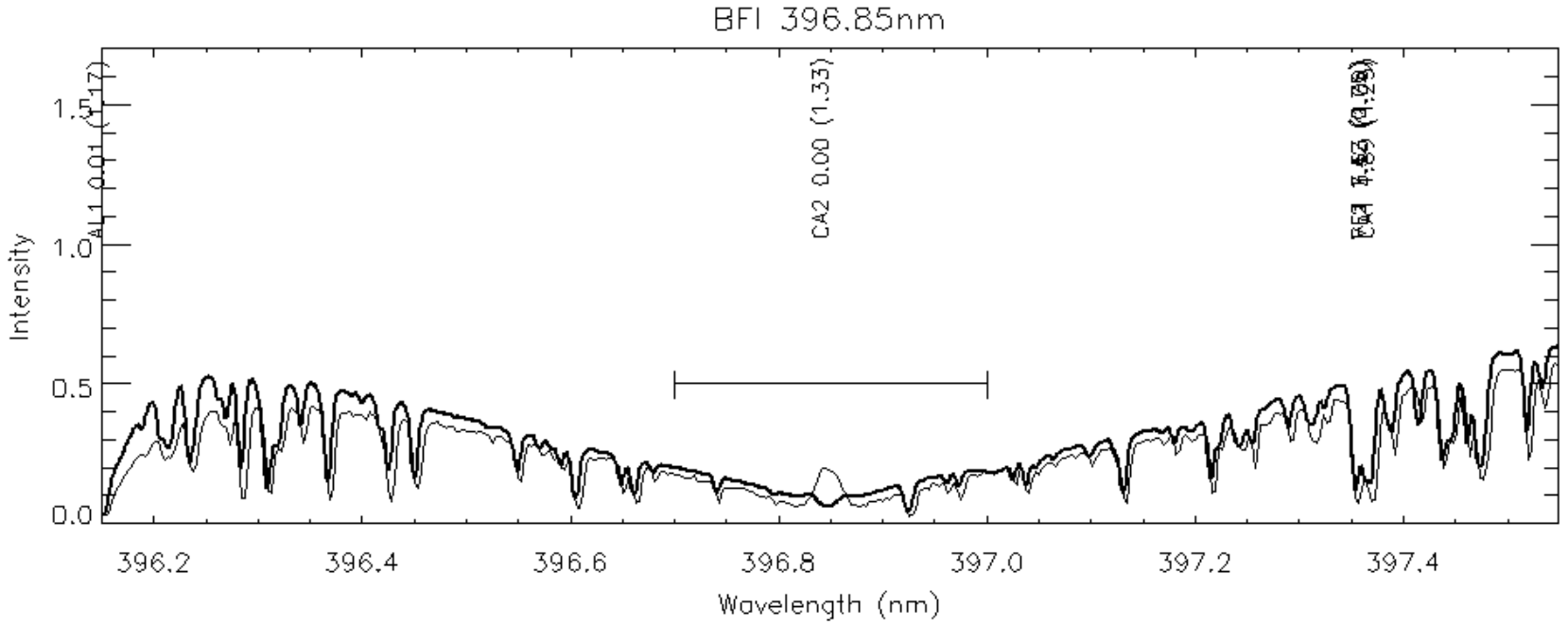
BFI 396.85nm
CA2 0.00 (1.33)
Intensity
Wavelength (nm)

BFI

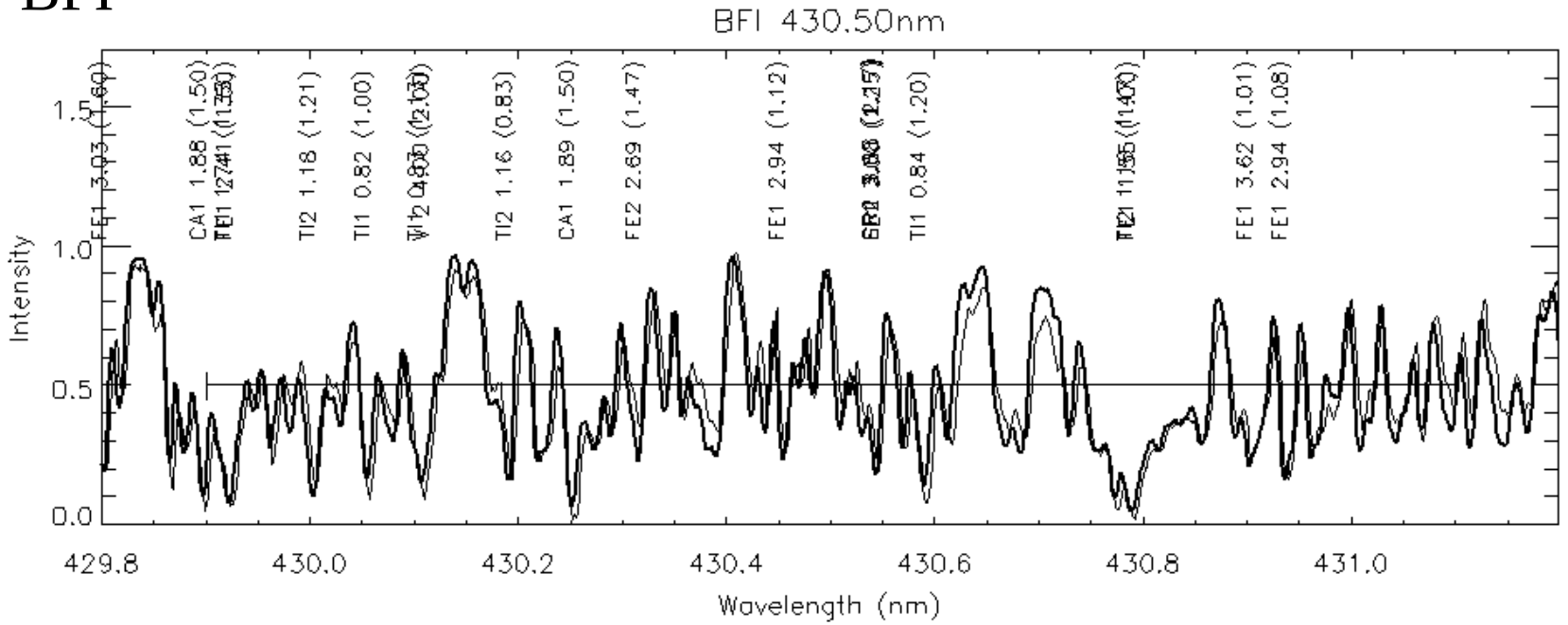
BFI 430.50nm
Intensity
Wavelength (nm)
429.8
430.0
430.2
430.4
430.6
430.8
431.0
0.0
0.5
1.0
1.5
CA1 1.89 (1.50)
TI2 1.18 (1.21)
TI1 0.82 (1.00)
TI2 1.16 (0.83)
CA1 1.89 (1.50)
FE2 2.69 (1.47)
FE1 2.94 (1.12)
TI1 0.84 (1.20)
FE1 3.62 (1.01)
FE1 2.94 (1.08)

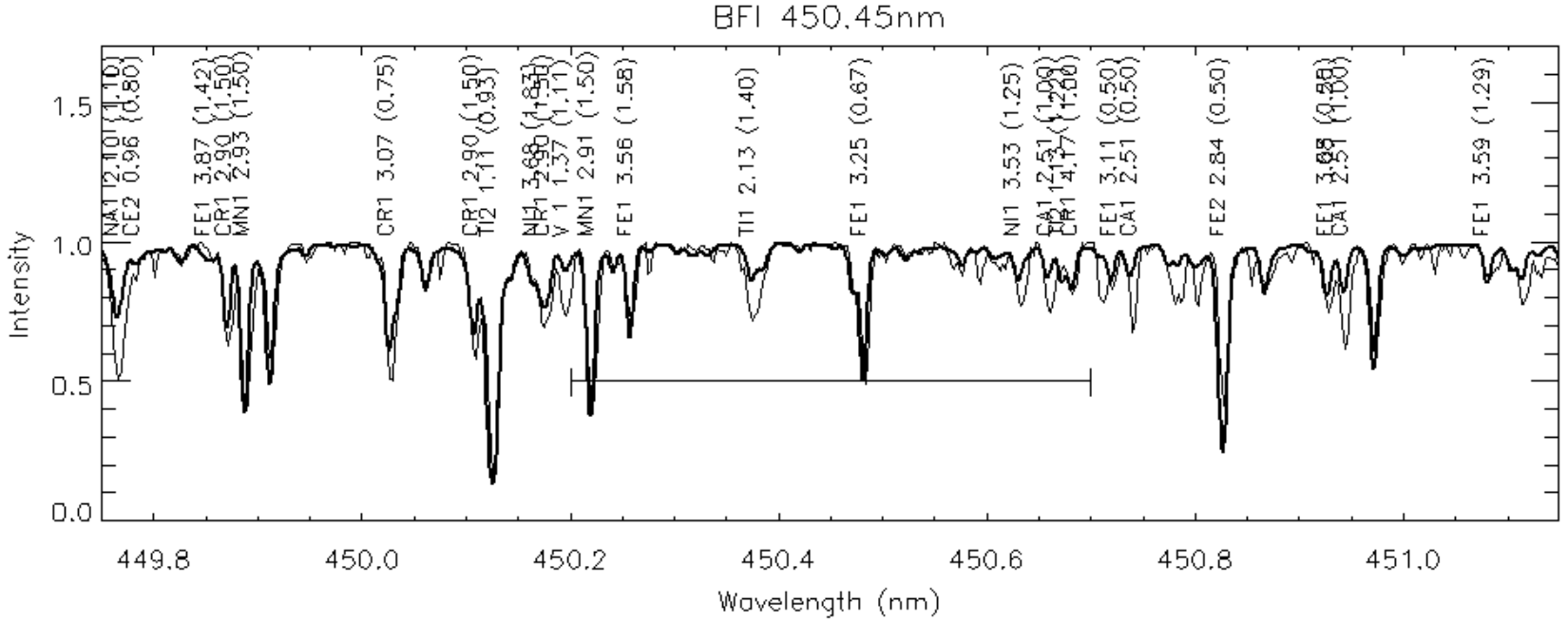
BFI 450.45nm
Intensity
Wavelength (nm)
449.8
450.0
450.2
450.4
450.6
450.8
451.0
0.0
0.5
1.0
1.5
FE1 3.87 (1.42)
CR1 2.90 (1.50)
MN1 2.93 (1.50)
CR1 3.07 (0.75)
CR1 2.90 (1.50)
TI2 1.11 (0.93)
MN1 2.91 (1.50)
FE1 3.56 (1.58)
TI1 2.13 (1.40)
FE1 3.25 (0.67)
NI1 3.53 (1.25)
FE1 3.11 (0.50)
CA1 2.51 (0.50)
FE2 2.84 (0.50)
FE1 3.59 (1.29)

BFI

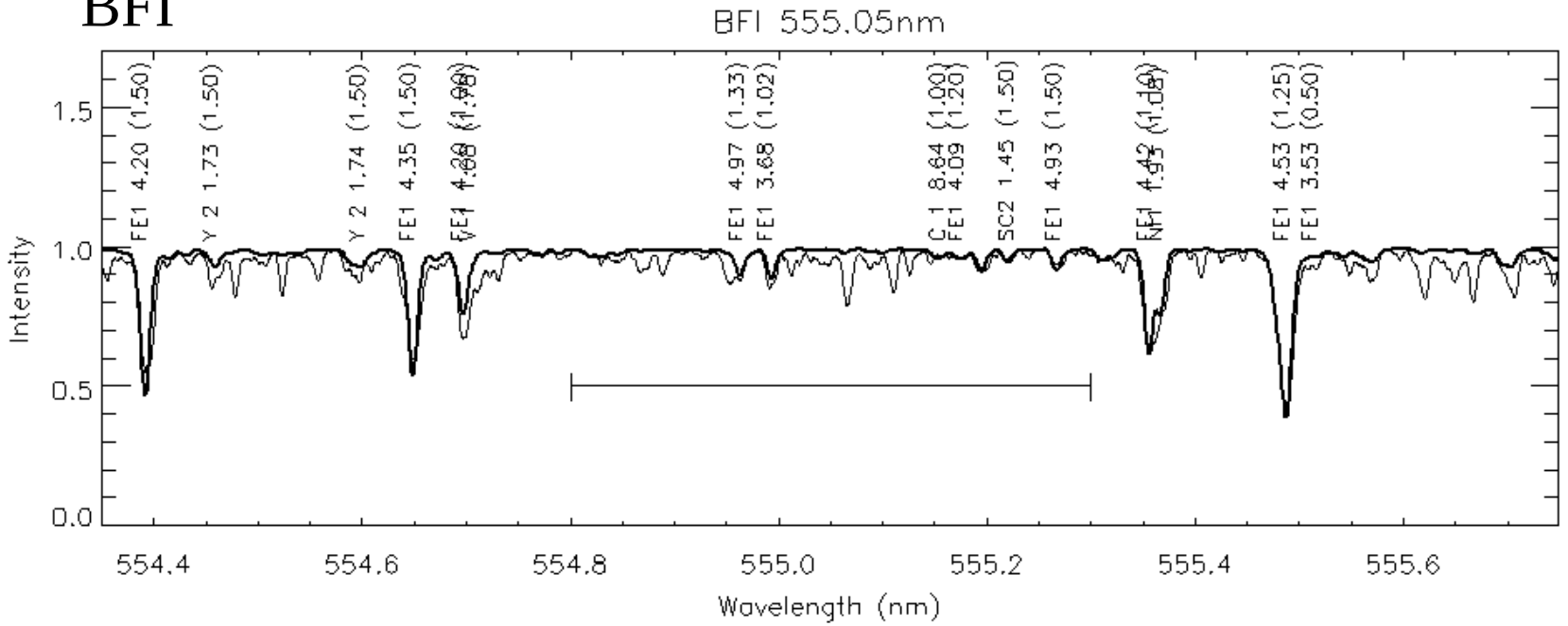
BFI 555.05nm
FE1 4.20 (1.50)
Y 2 1.73 (1.50)
Y 2 1.74 (1.50)
FE1 4.35 (1.50)
FE1 4.97 (1.33)
FE1 3.68 (1.02)
C 1 8.64 (1.00)
FE1 4.09 (1.20)
SC2 1.45 (1.50)
FE1 4.93 (1.50)
FE1 4.53 (1.25)
FE1 3.53 (0.50)
Intensity
Wavelength (nm)

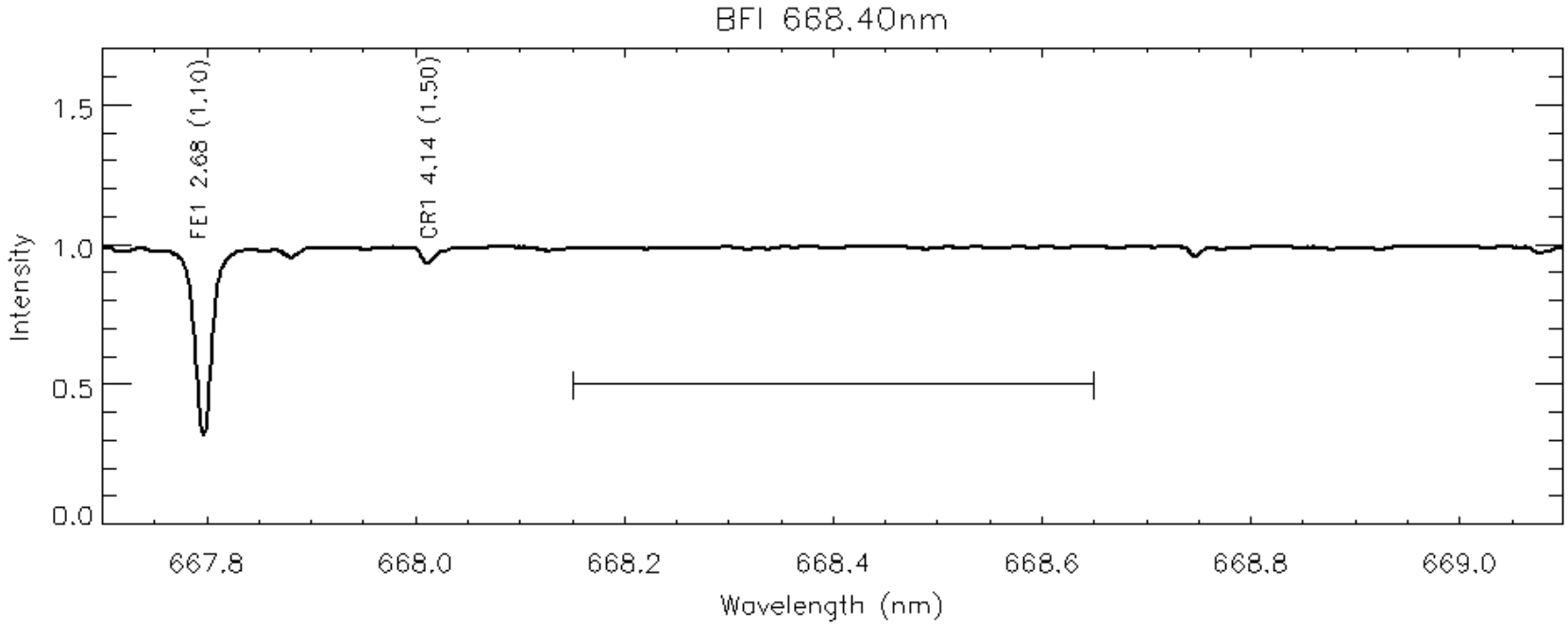
BFI 668.40nm
FE1 2.68 (1.10)
CR1 4.14 (1.50)
Intensity
Wavelength (nm)

Continuum contribution function

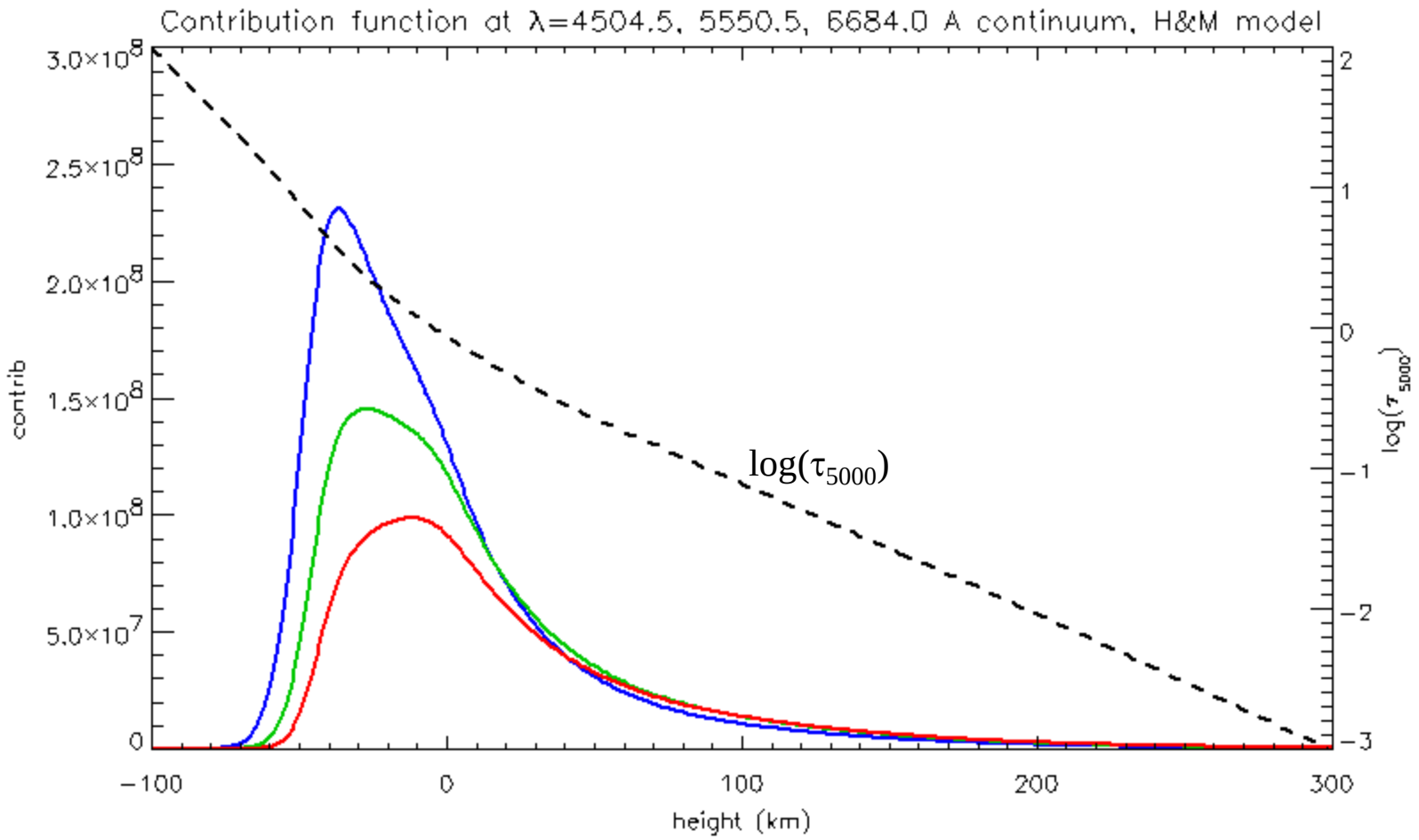

CH3883, CN4305 (G-band) の形成高さ

静穏領域

S. V. Berdyugina etal., 2003,
A&A 412, 513–527

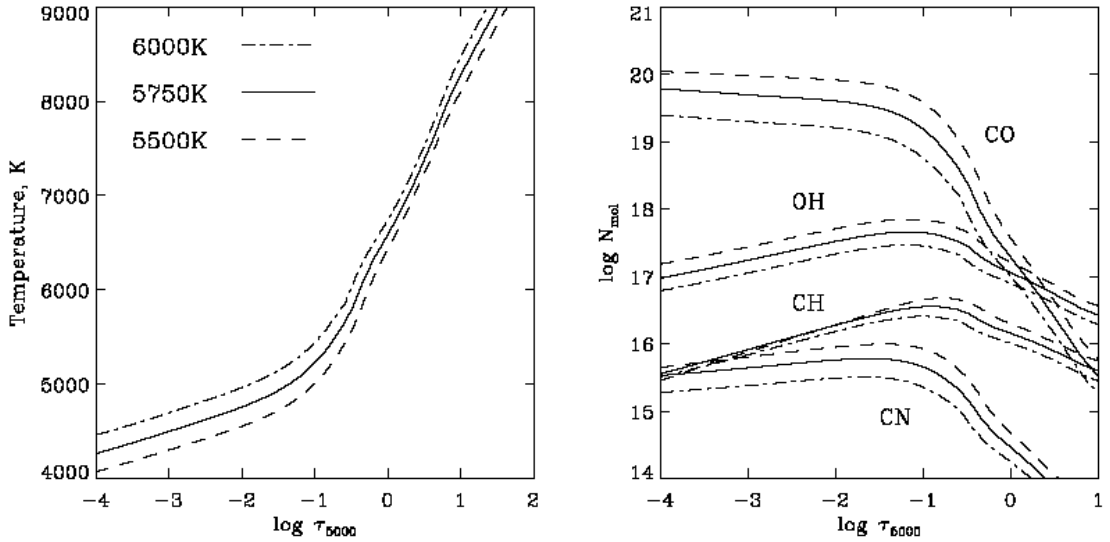

Fig. 9. On the left, temperature stratification of three atmospheric models by Kurucz (1993) with $T_{\rm eff}$ = 5750 ± 250 K representing the solar photosphere with temperature fluctuations. On the right, the corresponding number densities of 4 molecules relevant for these temperatures.

黒点

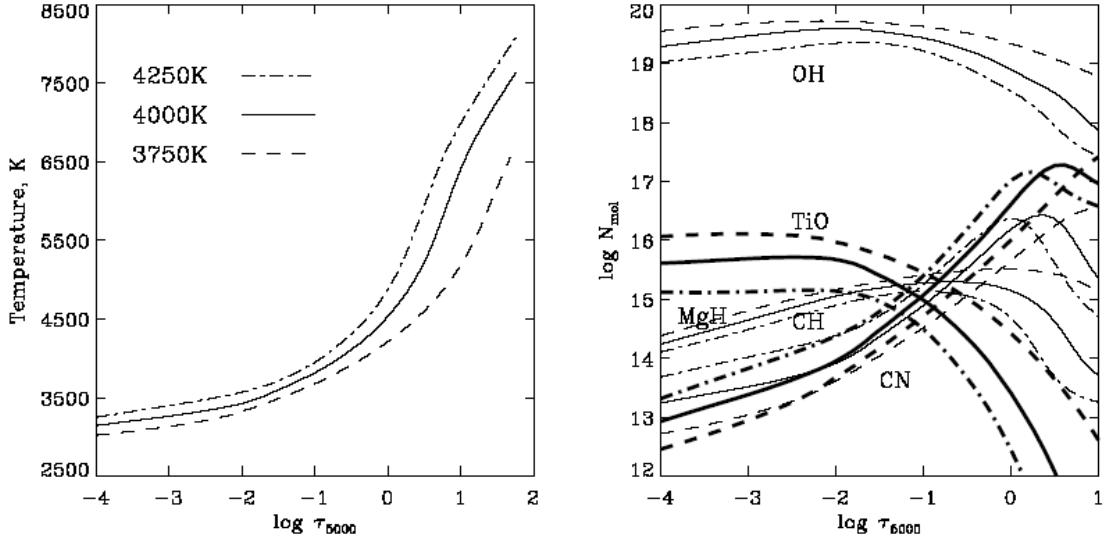

Fig. 10. On the left, temperature stratification of three models with $T_{\rm eff}$ = 4000 ± 250 K representing a sunspot or a cool stellar photosphere with temperature fluctuations. On the right, the corresponding molecular number densities. The curves representing TiO and CH are plotted thick in order to distinguish them from the curves representing MgH and CN.

NFI 517.27 (Mg b2)

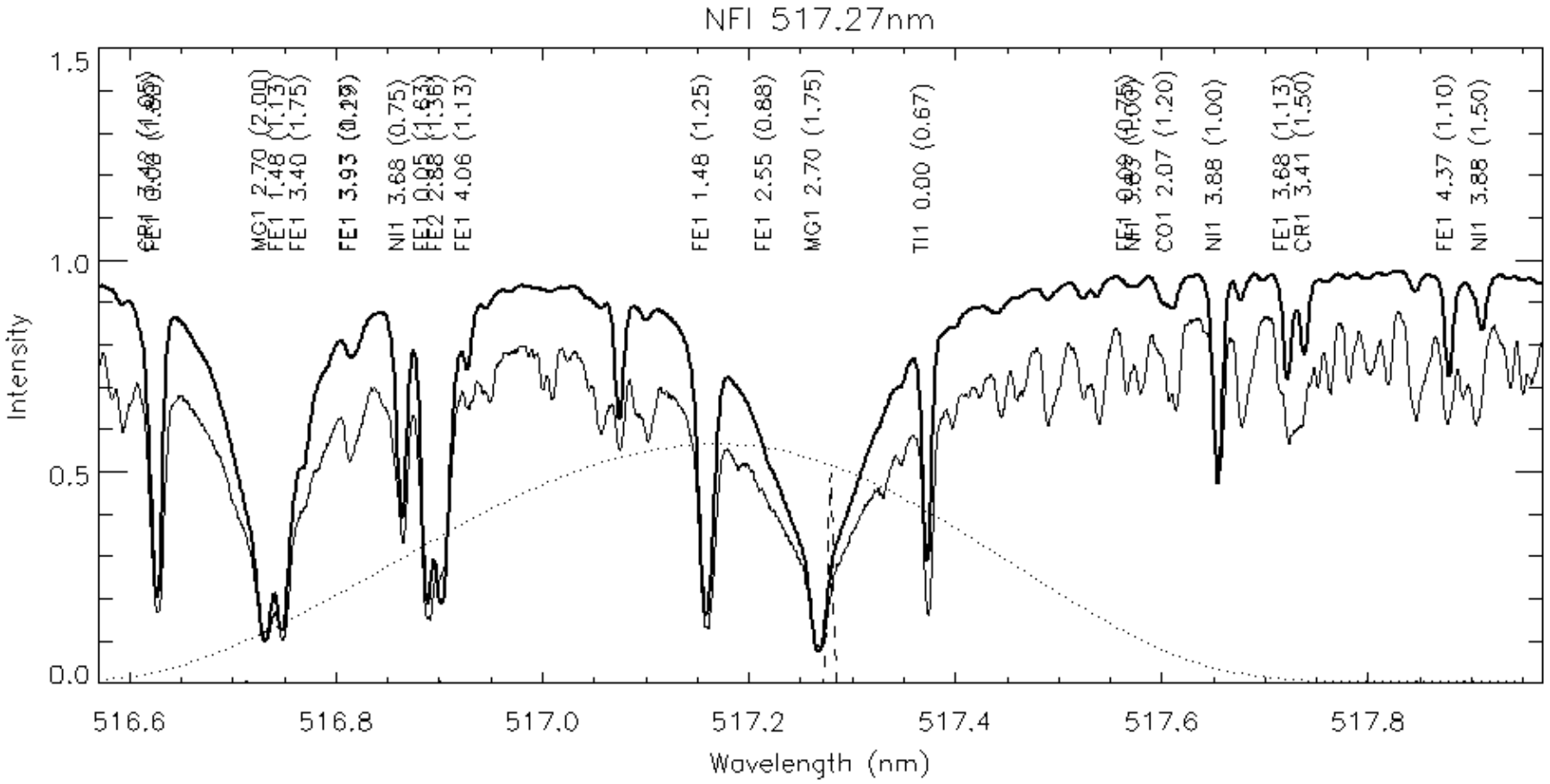

NFI 525.02

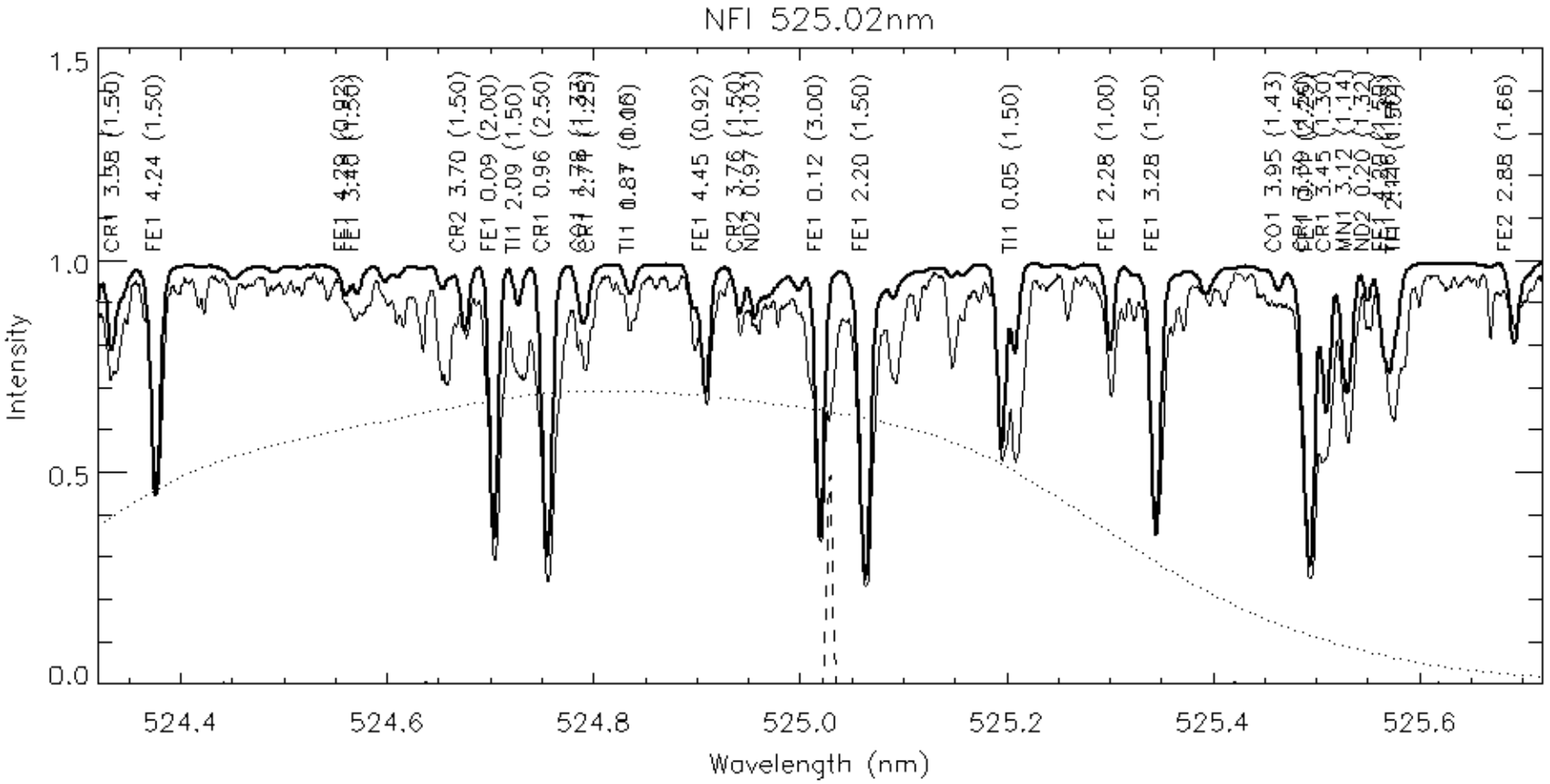
NFI 525.02nm
Intensity
Wavelength (nm)
1.5
1.0
0.5
0.0
524.4
524.6
524.8
525.0
525.2
525.4
525.6
CR1 3.58 (1.50)
FE1 4.24 (1.50)
CR2 3.70 (1.50)
FE1 0.09 (2.00)
TI1 2.09 (1.50)
CR1 0.96 (2.50)
FE1 4.45 (0.92)
CR2 3.76 (1.50)
ND2 0.97 (1.03)
FE1 0.12 (3.00)
FE1 2.20 (1.50)
TI1 0.05 (1.50)
FE1 2.28 (1.00)
FE1 3.28 (1.50)
CO1 3.95 (1.43)
CR1 3.45 (1.30)
MN1 3.12 (1.14)
ND2 0.20 (1.32)
FE2 2.88 (1.66)

NFI 557.60

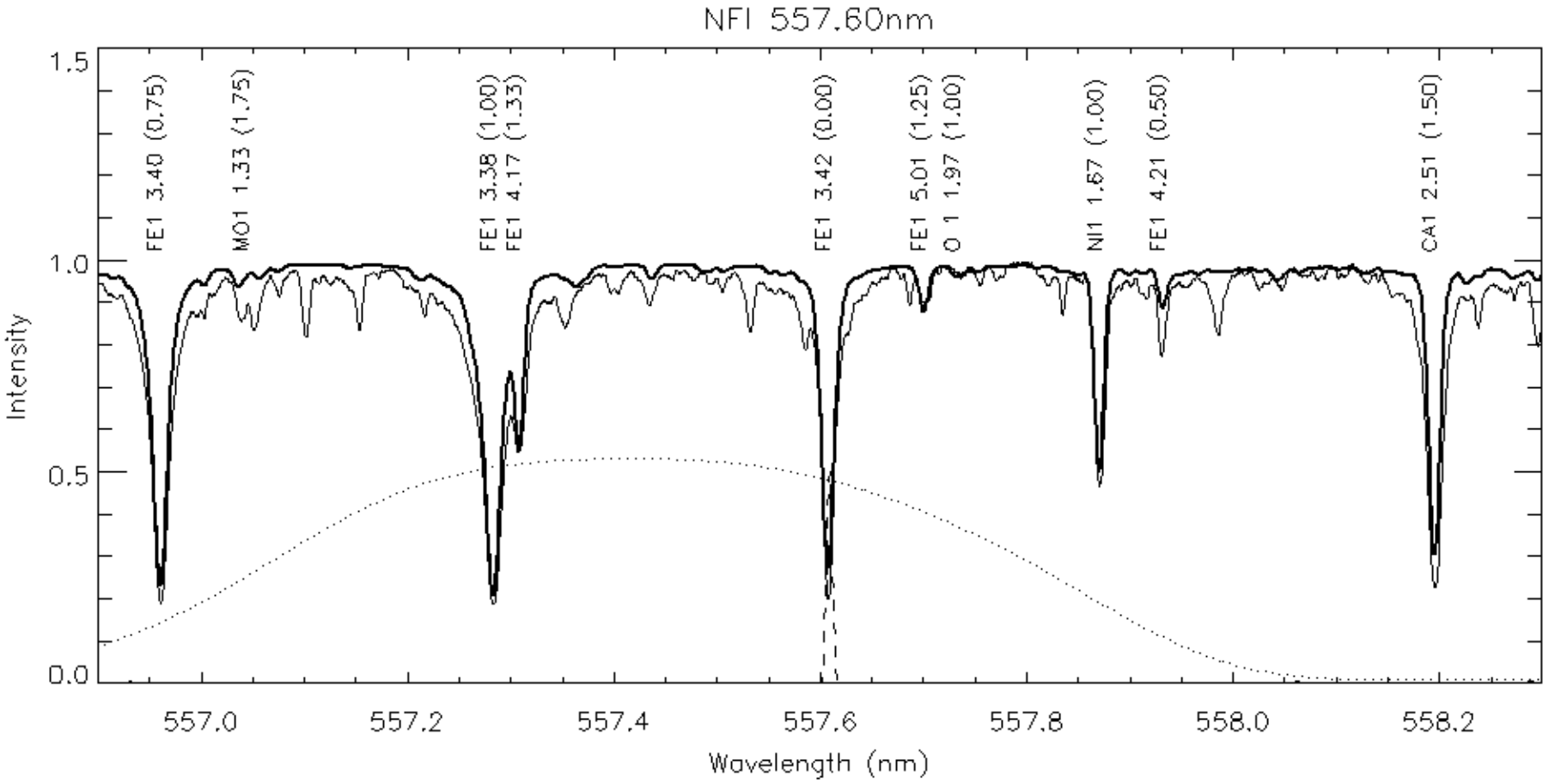
NFI 557.60nm
FE1 3.40 (0.75)
MO1 1.33 (1.75)
FE1 3.38 (1.00)
FE1 4.17 (1.33)
FE1 3.42 (0.00)
FE1 5.01 (1.25)
O 1 1.97 (1.00)
NI1 1.67 (1.00)
FE1 4.21 (0.50)
CA1 2.51 (1.50)
Intensity
1.5
1.0
0.5
0.0
557.0
557.2
557.4
557.6
557.8
558.0
558.2
Wavelength (nm)

NFI 589.60 Na D1

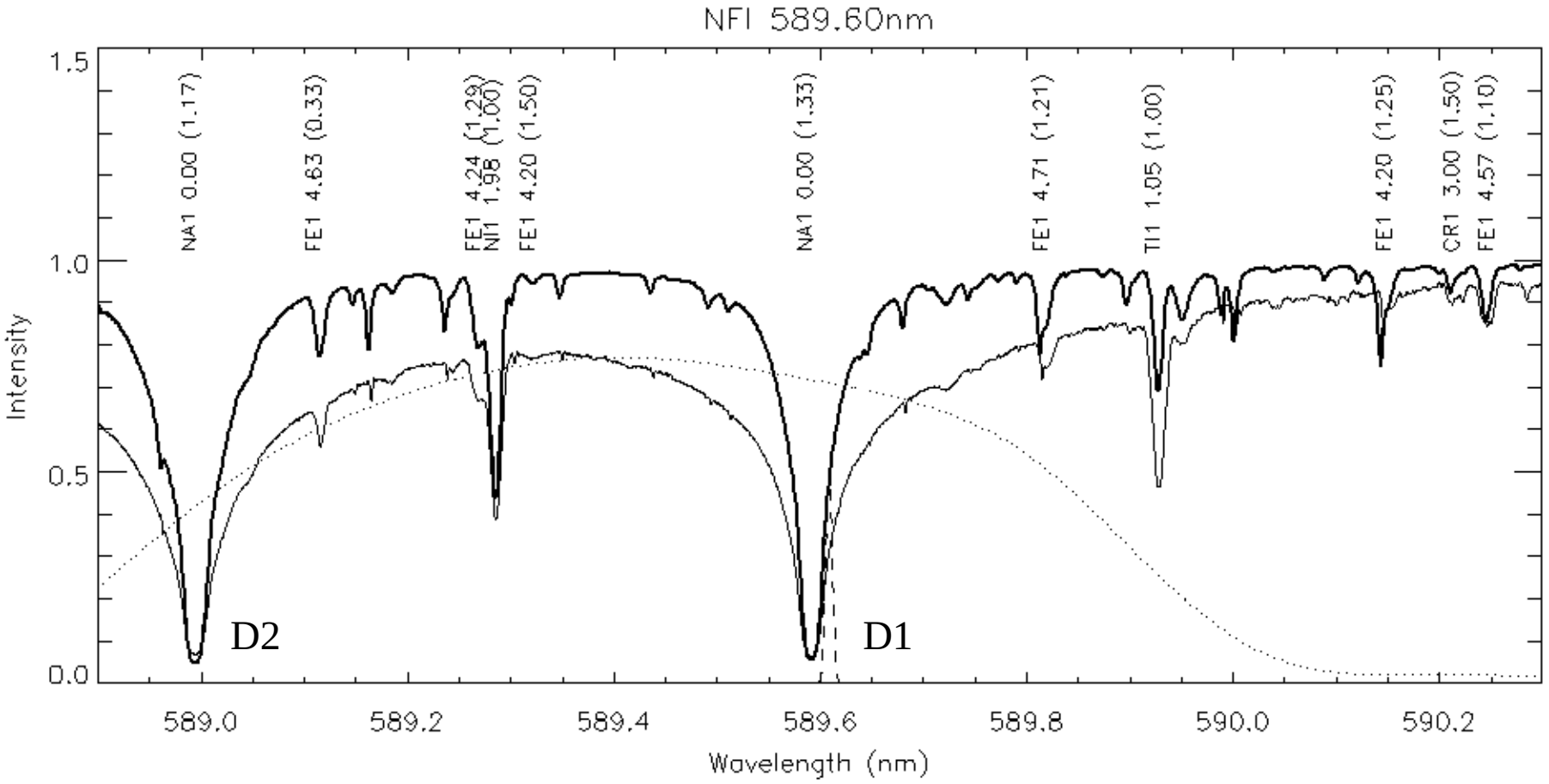

NFI 630.25

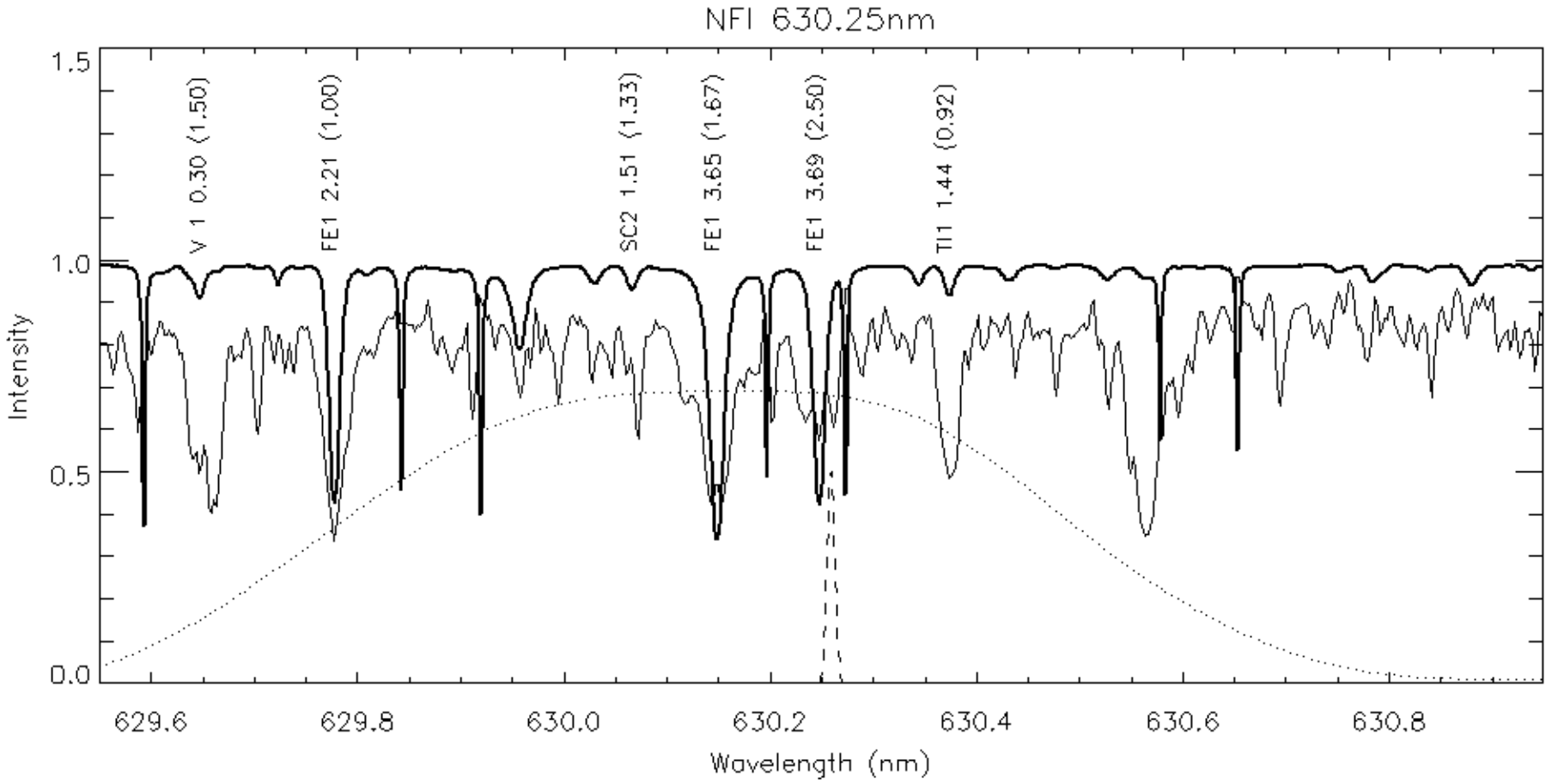
NFI 630.25nm
V 1 0.30 (1.50)
FE1 2.21 (1.00)
SC2 1.51 (1.33)
FE1 3.65 (1.67)
FE1 3.69 (2.50)
TI1 1.44 (0.92)
Intensity
1.5
1.0
0.5
0.0
629.6
629.8
630.0
630.2
630.4
630.6
630.8
Wavelength (nm)

NFI 656.27 Hα

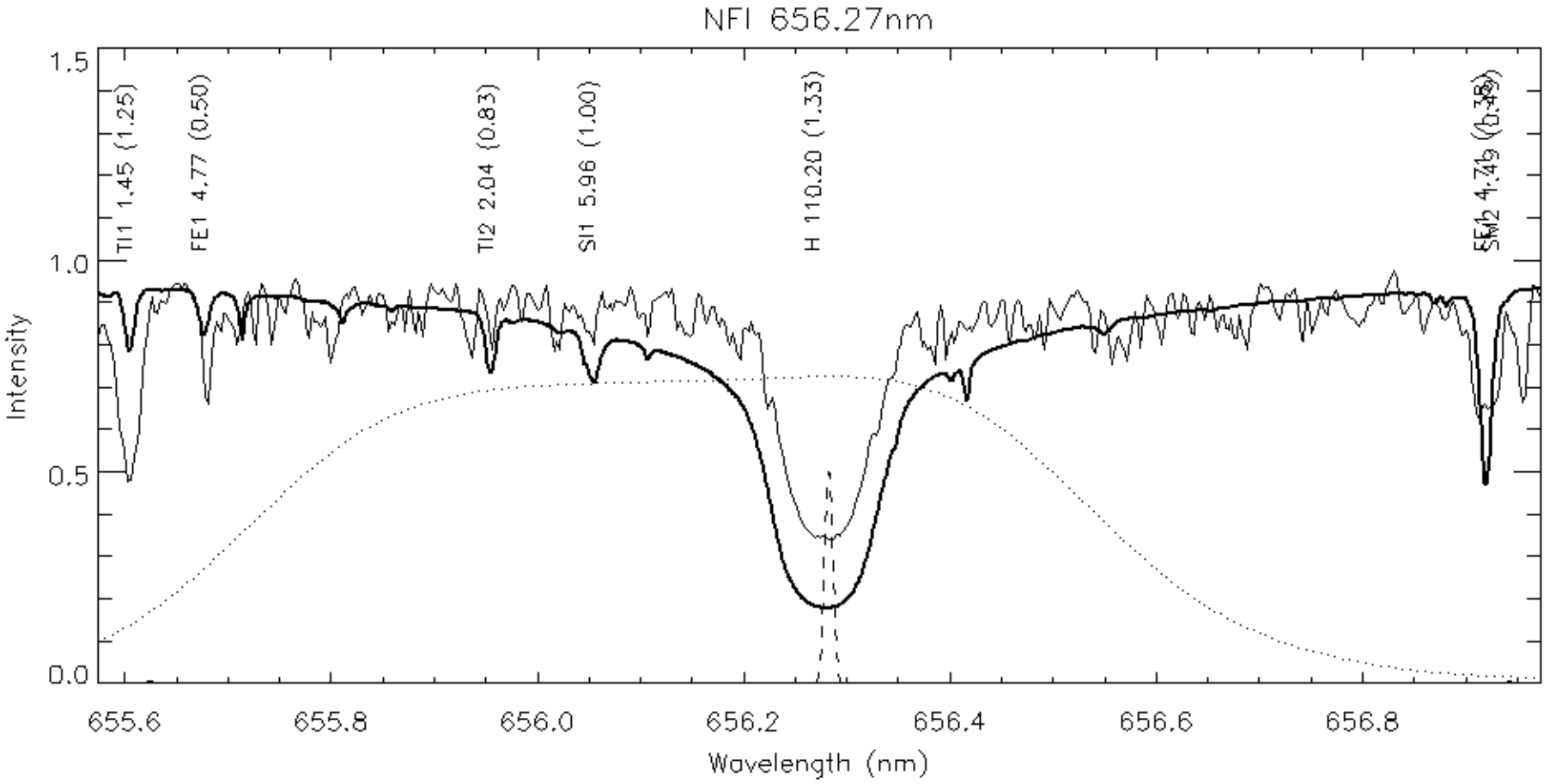
NFI 656.27nm
TI1 1.45 (1.25)
FE1 4.77 (0.50)
TI2 2.04 (0.83)
SI1 5.96 (1.00)
H 110.20 (1.33)
Intensity
1.5
1.0
0.5
0.0
655.6
655.8
656.0
656.2
656.4
656.6
656.8
Wavelength (nm)

MG1 5172.680 3P1 - 3S1 2.700 -.3800WI 1259.0 b2

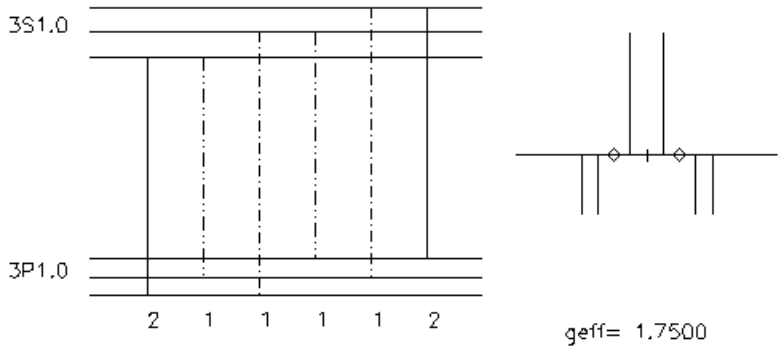

FE1 6302.503 5P1 - 5D0 3.686 -.6100CW 83.0

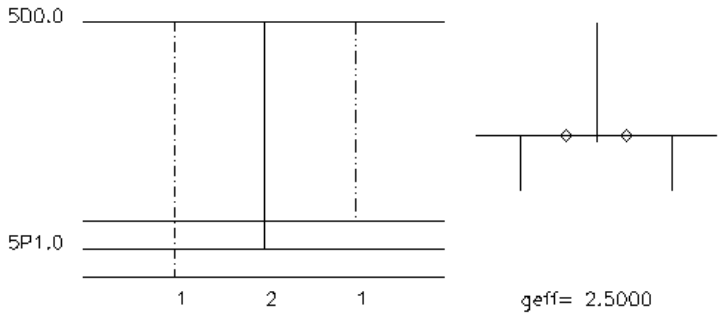

NA1 5895.920 2S0.5 - 2P0.5 .000 -.1840MS 564.0*

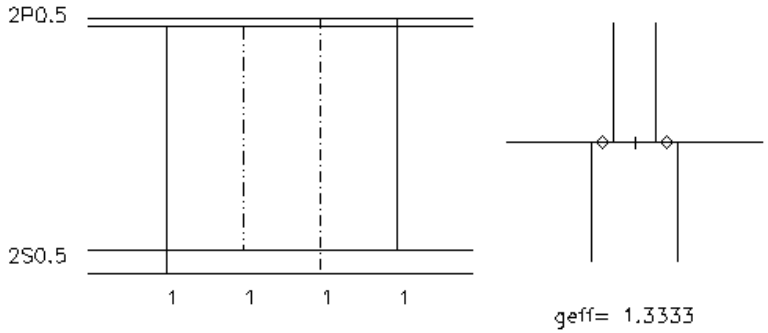

FE1 5250.207 5D0 - 7D1 .121 -4.4600CW 62.0

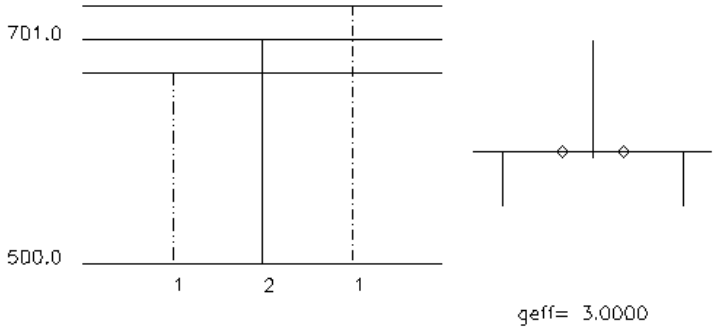

H 1 6562.740 1 2S 0.5 2P 0.5 10.199 -.0606WI 4020.0

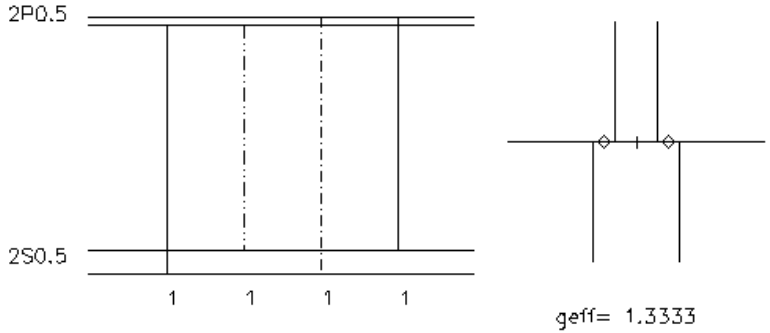

偏光サンプリング

16点連続サンプリング

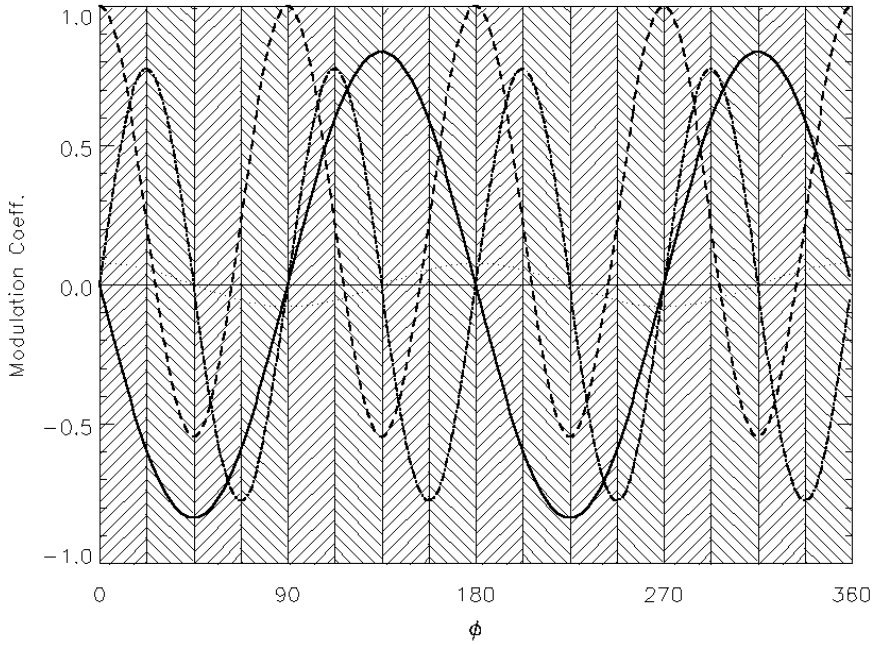

SP
NFI シャッターレスモード
変調サイクル = 0.8sec ➔ ε ~ 0.1%

4点間欠サンプリング（例）

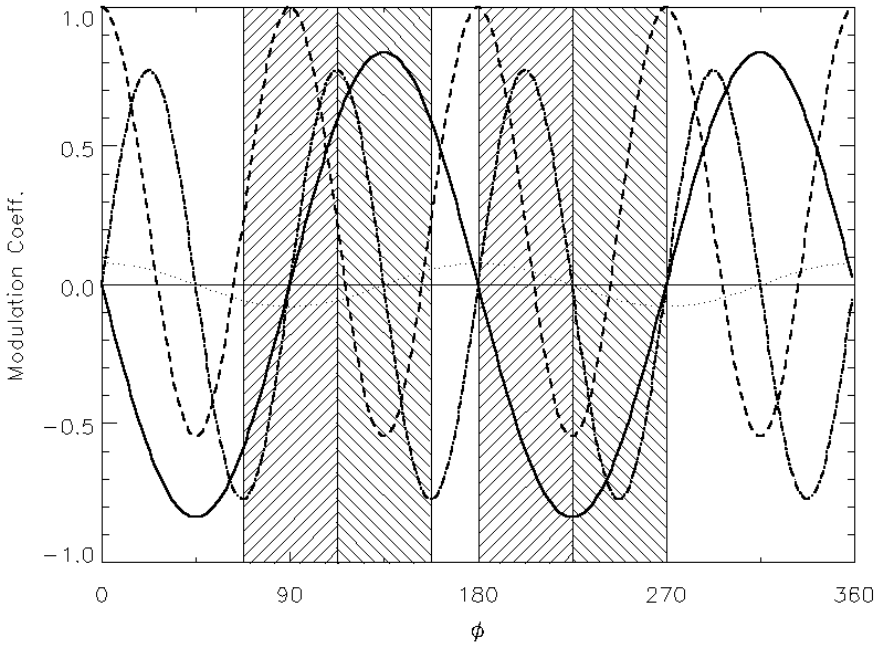

NFI シャッターモード
変調サイクル > 5sec ➔ ε ~ 0.5%

机上デモジュレーション・積算

NFIシャッターレスモード

焦点面マスクで視野を限定し、メカニカルシャッターを用いずに中心部画像を連続読み出し(10Hz)するモード。
読み出した画像はSPと同様機上積算・デモジュレーションが施される。

FG CCD

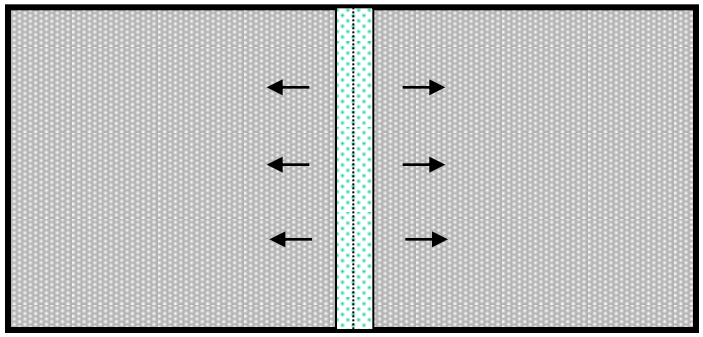

焦点面マスクの視野

16” x 163.8”
32” x 163.8”
64” x 163.8”
128” x 163.8”
164” x 163.8”
328” x 163.8”

SOTの偏光キャリブレーション　　2005.6 @三鷹

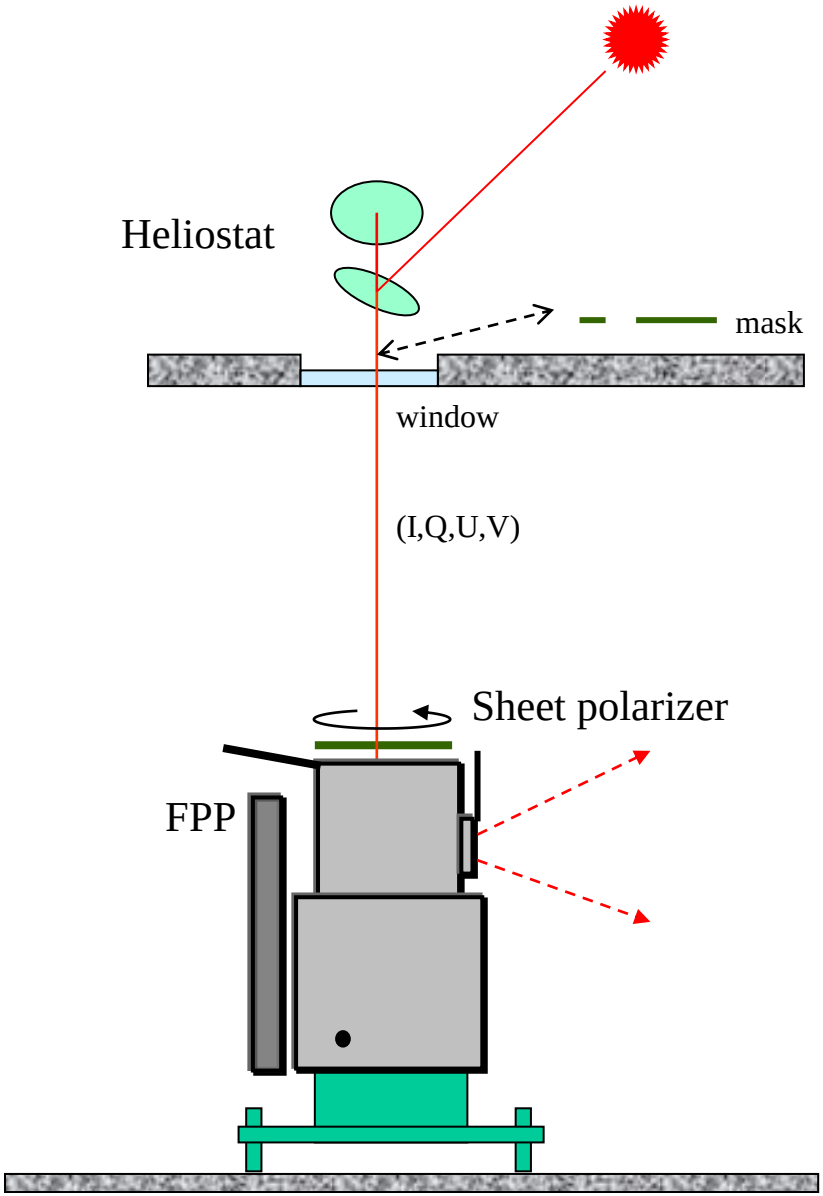

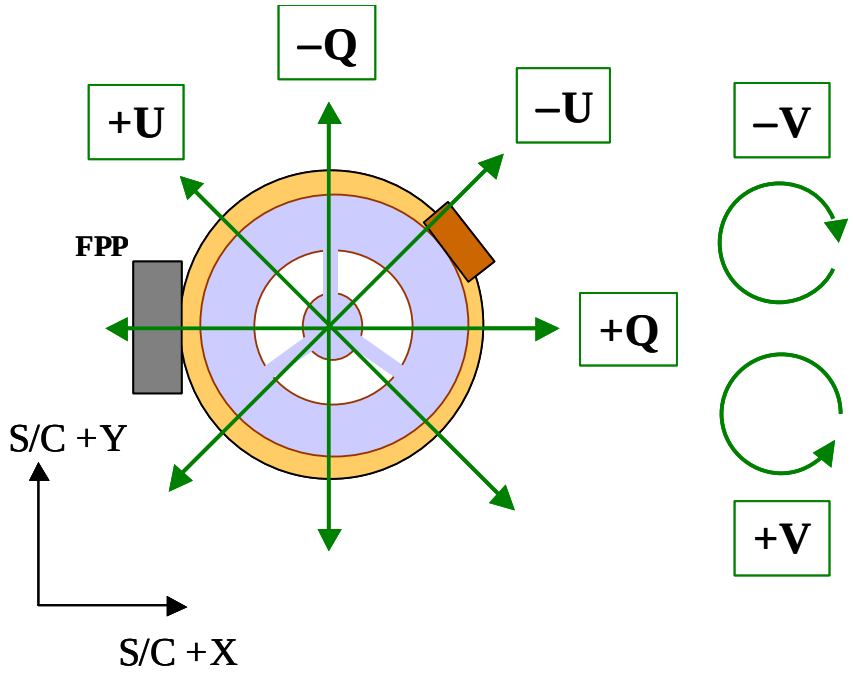

View from the top of SOT

FPPから出てくる(IQUV)と入射光の(IQUV)を関係付ける
Xマトリックスを取得。

$$\begin{pmatrix} I \\ Q \\ U \\ V \end{pmatrix}_{product} = \begin{pmatrix} x_{00} & x_{10} & x_{20} & x_{30} \\ x_{01} & x_{11} & x_{21} & x_{31} \\ x_{02} & x_{12} & x_{22} & x_{32} \\ x_{03} & x_{13} & x_{23} & x_{33} \end{pmatrix} \begin{pmatrix} I \\ Q \\ U \\ V \end{pmatrix}_{incident}$$

精度　➔ 0.001% の測定でクロストークが見えない精度

–	0.3333	0.3333	0.2500
0.0010	0.0500	0.0067	0.0050
0.0010	0.0067	0.0500	0.0050
0.0010	0.0067	0.0067	0.0500

SP

x matrices at scan center; CCD image

each element is scaled to median $\pm$ tolerance, x_{00} (=1) is replaced by *I*-image

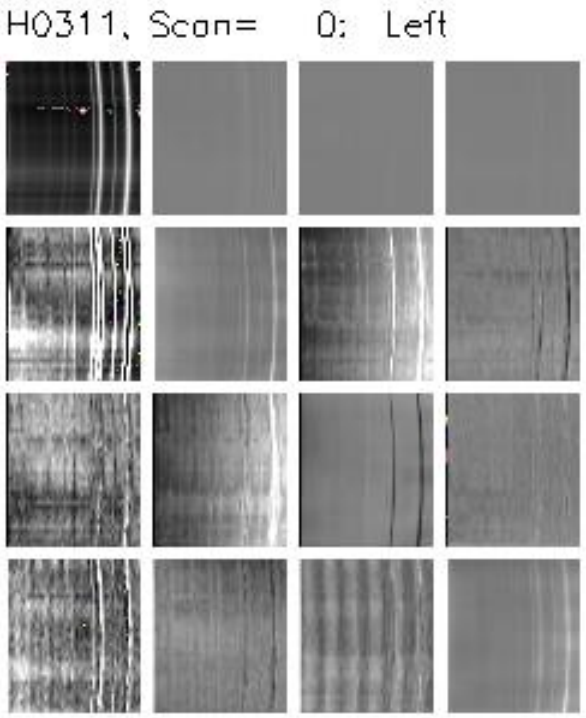

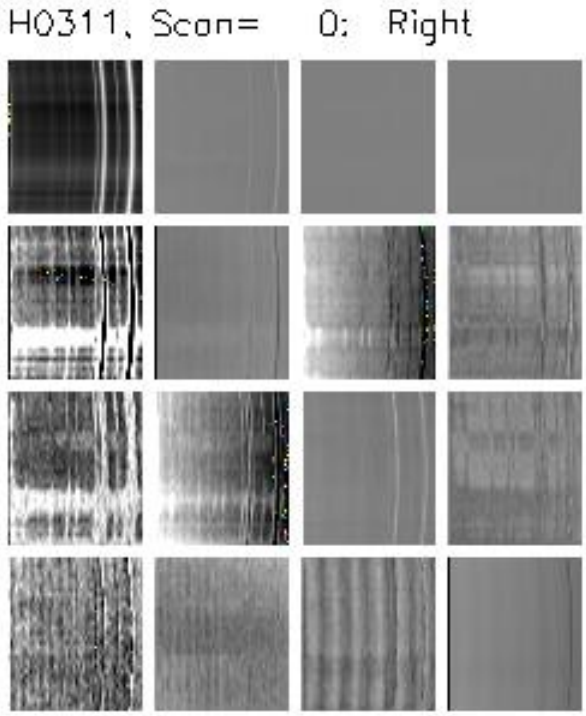

Median Mueller matrix

Left

1.0000	0.2205	0.0187	-0.0047
0.0012	0.4813	0.0652	-0.0014
0.0001	0.0513	-0.4803	-0.0057
-0.0025	0.0032	-0.0046	0.5256

Right

1.0000	-0.2112	-0.0170	-0.0051
-0.0025	-0.4875	-0.0560	0.0022
-0.0001	-0.0426	0.4907	0.0060
0.0027	-0.0008	0.0042	-0.5301

The x matrix can be regarded as constant in the CCD.

x-matrix elements against the scan position

Each point is the median in the CCD, scale = average $\pm$ 0.01,
dotted horizontal lines show tolerances for each element

Asterisk: Left CCD
Diamond: right CCD

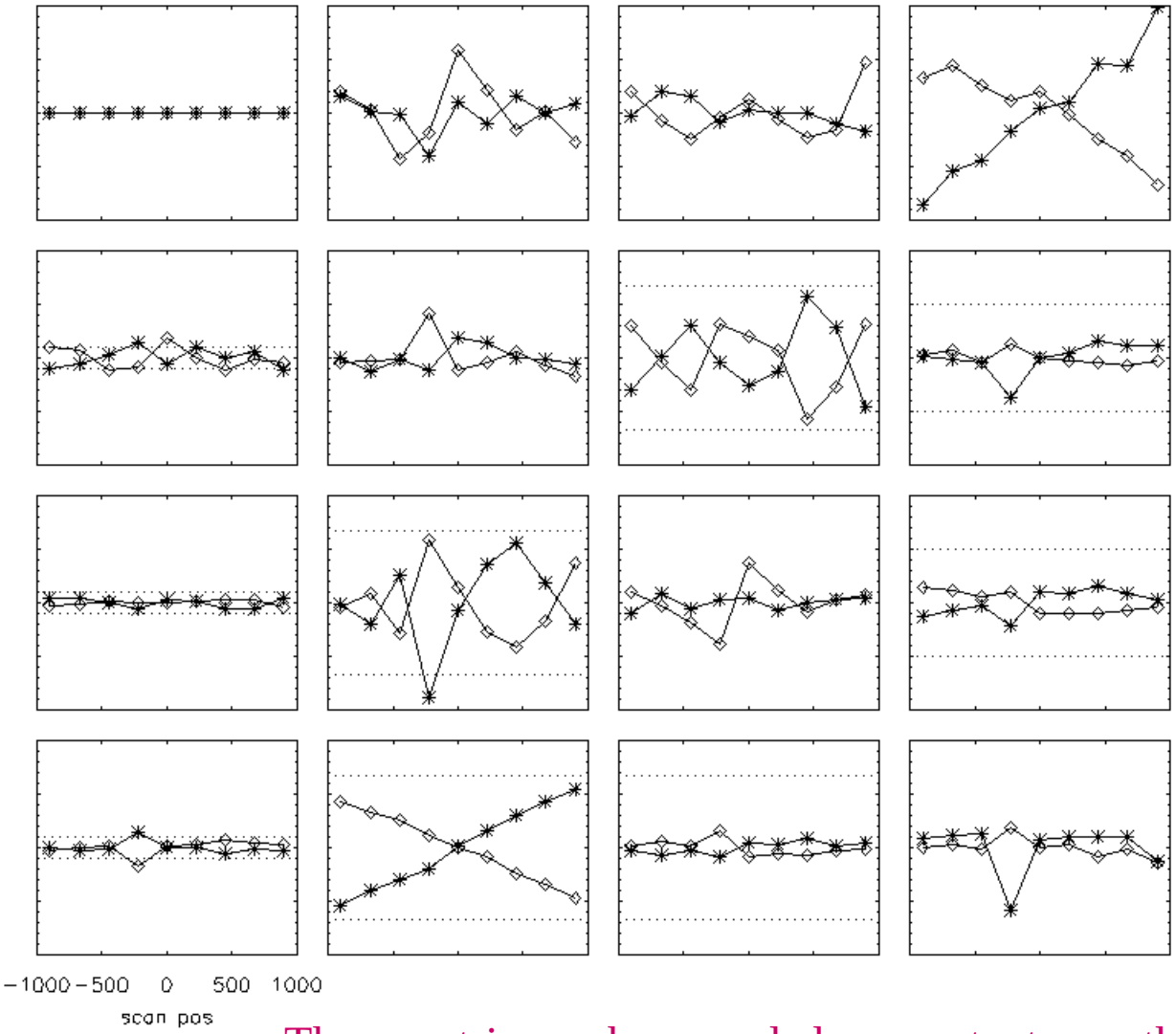

The x matrix can be regarded as constant over the scan position

FG/NFI の例

X matrix over the CCD, 5172

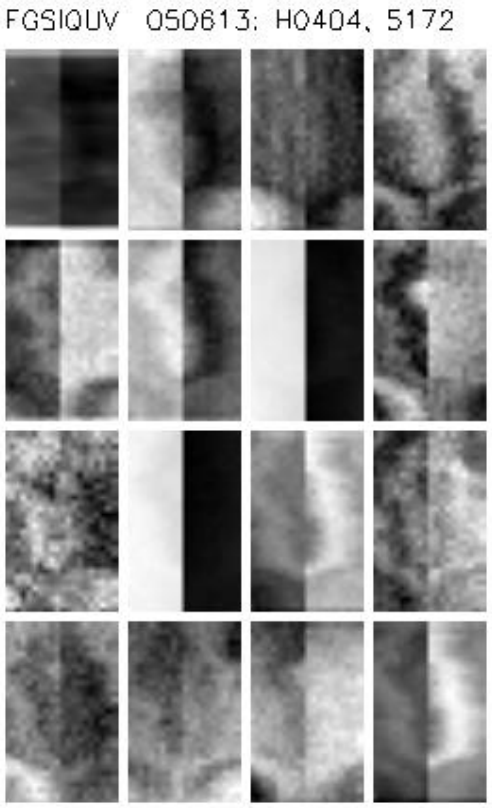

80x1024

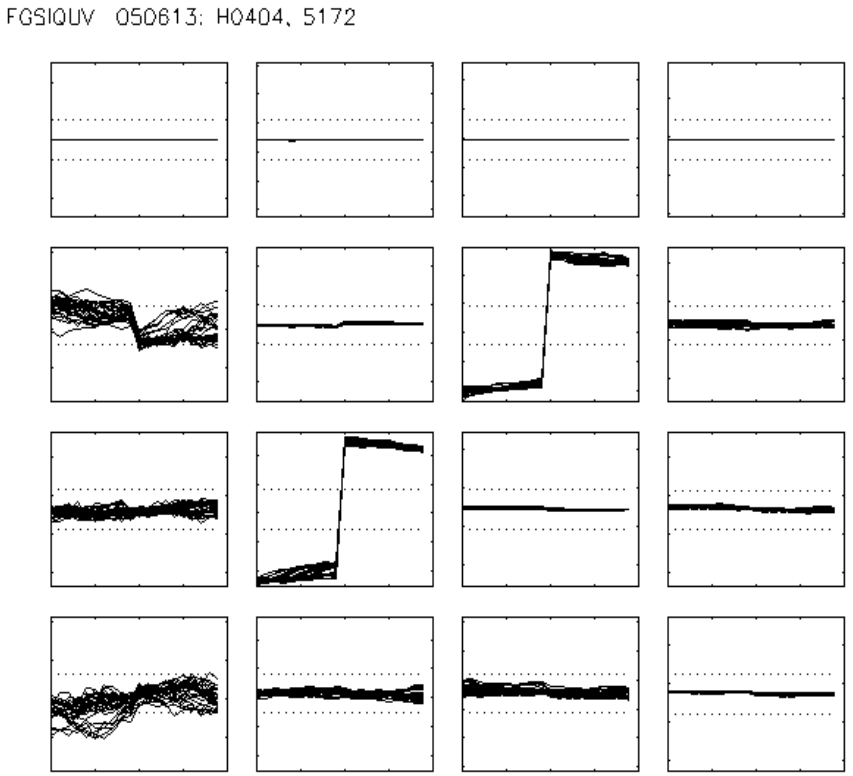

left: theta= -1.571deg.

1.0000	-0.2994	-0.0336	-0.0435
0.0009	-0.4544	0.0208	0.0045
-0.0009	0.0287	0.4478	0.0068
-0.0085	0.0318	-0.0134	0.5774

right: theta= -4.441deg.

1.0000	-0.2871	-0.0305	-0.0434
-0.0003	-0.4473	0.0653	0.0038
-0.0007	0.0738	0.4435	0.0061
-0.0077	0.0310	-0.0150	0.5718

各波長における偏光モジュレーションの大きさ

PMUの遅延量

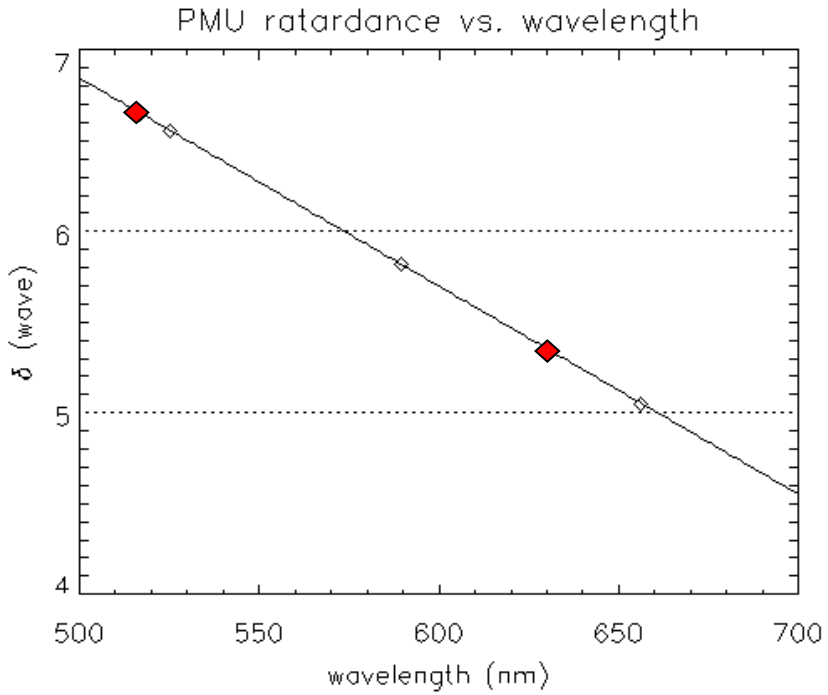

Wavelength (nm)	Designed Retardation (wave)	Theoretical Modulation amplitude		Measured sensitivity (Diagonal element of x-matrix)		
		QU	V	QU	V	Q→I
517.2	6.650	0.79	0.81	0.452	0.577	0.297
525.0	6.558	0.97	0.36	0.609	0.266	0.049
589.6	5.816	0.30	0.91	0.297	0.633	0.531
630.2	5.350	0.79	0.81	0.503	0.526	0.218
656.3	5.050	0.03	0.31	0.073	0.402	0.882

NFI 弱い磁場の検出限界

1) Diagonal elements of x-matrix give the polarization sensitivity of SOT

$Q_p \sim x_{11} Q_z$

$V_p \sim x_{33} V_z$

Q_z, V_z are Zeeman signal in spectral line

Q_p, V_p are SOT response

2) Detection limit of Q_p, V_p are given by the photometric accuracy in spectral line

$$\varepsilon' = \sqrt{\frac{I_c}{I_{line}}}\,\varepsilon$$

ε is photometric accuracy in continuum

~ 0.001

3) Week Zeeman singnal (Q_z, V_z) can crudely be given by the assumption of that the Zeeman effect is a simple separation of I-profile

$$Q \sim \left(\alpha g_{eff} \lambda^2 B_\perp\right)^2 \left|\frac{d^2 I'}{d\lambda^2}\right|_{\max}$$

$$V \sim \alpha g_{eff} \lambda^2 B_{//} \left|\frac{dI'}{d\lambda}\right|_{\max},$$

$$I' = I(\lambda) \otimes T(\lambda)$$

Line profile convoluted with the tunable filter profile

4) Thus detection limit for magnetic fields are given

$$\Delta B_{//} \sim \frac{1}{x_{33}} \sqrt{\frac{I_c}{I_{line}}}\, \frac{1}{\alpha g_{eff} \lambda^2 \left|dI'/d\lambda\right|_{\max}}\, \varepsilon$$

$$\Delta\left(B_\perp\right)^2 \sim \frac{1}{x_{11}} \sqrt{\frac{I_c}{I_{line}}}\, \frac{1}{\left(\alpha g_{eff} \lambda^2\right)^2 \left|d^2 I'/d\lambda^2\right|_{\max}}\, \varepsilon$$

Detection limit of NFI for weak magnetic fields, $\varepsilon = 0.001$

Wavelength (nm)	g_{eff}	Pol. Sensitivity (diagonal element of x)		Detection limit for B (Gauss)	
		V	QU	B_l	B_t
517.2	1.75	0.577	0.452	86	656
525.0	3.00	0.266	0.609	18	106
557.6	0.00	-	-	-	-
589.6	1.33	0.633	0.297	40	(670)
630.2	2.50	0.526	0.503	12	122
656.3	1.33	0.402	0.073	119	>2000

フィルターグラフによる磁場定量解析の可能性

モデルストークスプロファイルによるFG観測のシミュレーション

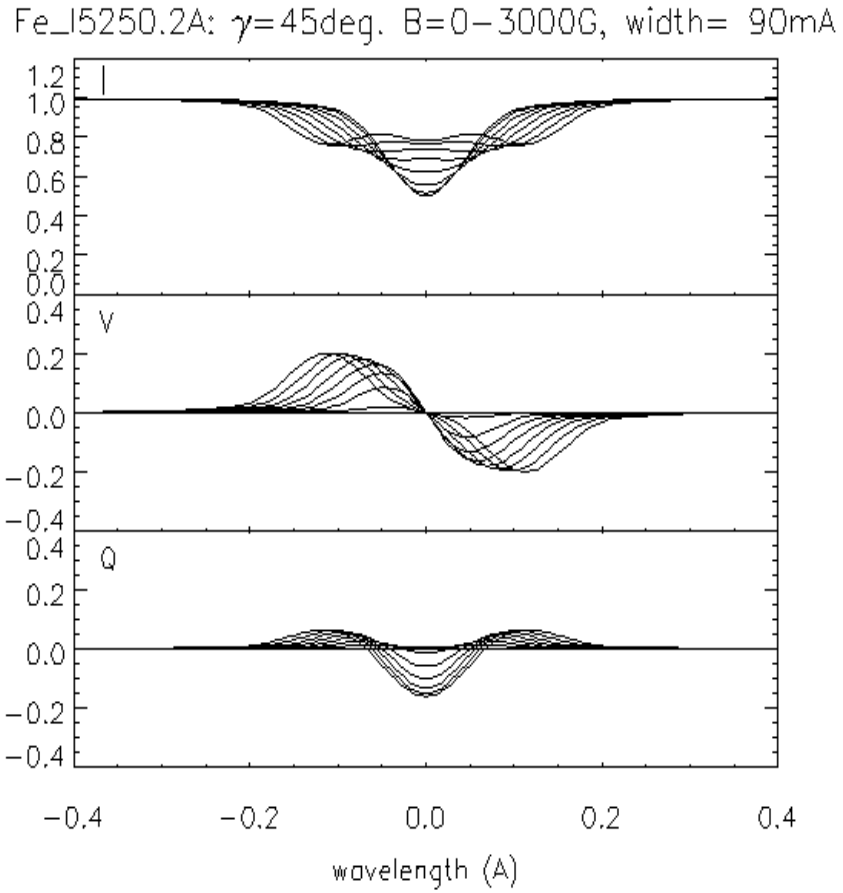

Stokes profile synthesis

- Model atmospheres (LTE)
  - Standard: Holweger&Muller (1974)
  - Spot : T = T – 1000K
  - Turbulent region: Vt = Vt × 2.
- Line: FeI 5250.2A, g_{eff} = 3.0, Ep = 0.12 eV
- Uniform velocity (symmetric profile only)
  v= –2.3~ +2.3 km/s (line shift –40 ~+40 mA)
- B= 0 – 3000G
- γ = 10, 45, 80° (angle between B and LOS)
- χ = 0° (azimuth angle of B)

NFI observable synthesis

- Filter width = 90 mA
- # of sampling points = 1, 2, 4

‘Stokes inversion’ with the NFI observable, (I_i, Q_i, U_i, V_i)

N= # of wavelength taken by NFI, *i* stands for the wavelength position.

N=1, $\Delta\lambda = -80$ mA

$V_{\text{index}} = V_1/I_1$

$Q_{\text{index}} = Q_1/I_1$

S_{index} = no Doppler information

N=2, $\Delta\lambda = -80, +80$ mA

$V_{\text{index}} = (V_1 - V_2) / (I_1 + I_2)$

$Q_{\text{index}} = (Q_1 + Q_2) / (I_1 + I_2)$

$S_{\text{index}} = (I_1 - I_2) / (I_1 + I_2)$

N=4, $\Delta\lambda = -120, -40, +40, +120$ mA (uniform spacing)

$V_{\text{index}} = (S^+ - S^-)/2$

$S^{\pm} = \text{c tan}^{-1}\{(I_3^{\pm} - I_1^{\pm} + I_4^{\pm} - I_2^{\pm}) / (I_1^{\pm} - I_2^{\pm} - I_3^{\pm} + I_4^{\pm})\}, \quad I_i^{\pm} = I_i \pm V_i$

$Q_{\text{index}} = \{Q_{\text{blue}}(\lambda_2 - \lambda_1)/(I_1 - I_2) + Q_{\text{red}}(\lambda_4 - \lambda_3)/(I_4 - I_3)\} / 2$

$Q_{\text{blue}} = \{(Q_1^2 + Q_2^2)/2\}^{1/2}, \quad Q_{\text{red}} = \{(Q_3^2 + Q_4^2)/2\}^{1/2}$

$S_{\text{index}} = \text{c tan}^{-1}\{(I_3 - I_1 + I_4 - I_2) / (I_1 - I_2 - I_3 + I_4)\}$

N=4, $\Delta\lambda = -110, -70, +70, +110$ mA (non-uniform spacing)

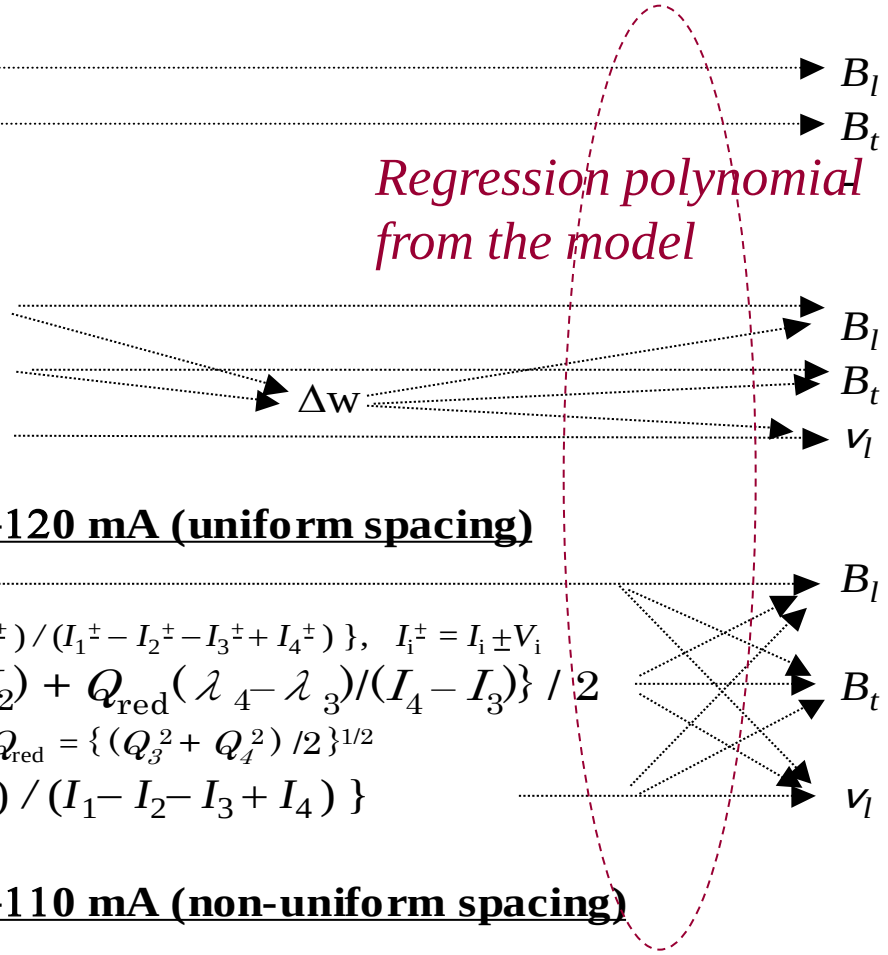

Basically the same (**cos** fitting), but a little more sophisticated algorithm.

N = 1
Δλ = –80mA

N = 2
Δλ = ± 80mA

N = 4,
uniform λ step
Δλ = –120 ,–40,
+40, +120 mA

N = 4,
non-uniform λ step
Δλ = –110 ,–70,
+70, +110 mA

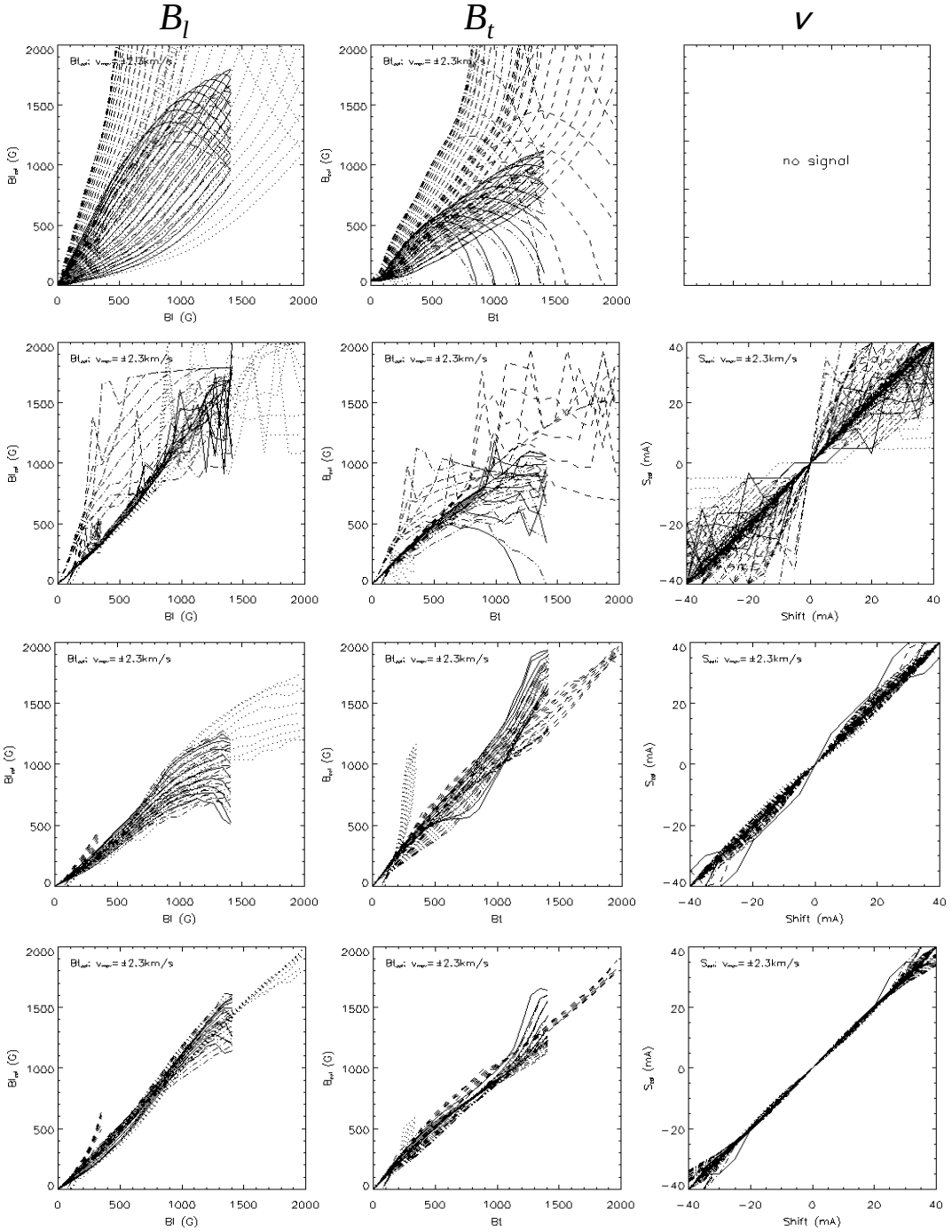

NFI の使い方

メリット：２次元画像・高時間分解能
FGでも４波長観測をすることによりある程度磁場の定量解析は可能、
ただし磁場の弱い領域はshutterless modeでないと苦しい。

波長 (A)	用途	磁場検出限界 0.1% (G)	
		B_l	B_t
5172	黒点領域彩層底部ベクトル磁場 黒点外だとかなりがんばって積算が必要 （フォトン数が厳しい、積算しても空間分解能が落ちないところはみそ）	86	656
5250	ベクトル磁場取得（6302よりも空間分解能が高い） 5247と組み合わせてfilling factor の診断 6302と組み合わせて光球深さ構造？	18	106
5576	光球速度場を少ない露光（高い時間分解能）で取得	-	-
5896	円偏光が得意 Vモードで視線方向磁場取得（Q→Iクロストークは小さいはず） 光球磁場と合わせて dBz/dz 導出 プロミネンスコアの密度、磁場診断	40	(670)
6302	光球ベクトル磁場、SPと相補的な使い方 6301と組み合わせてfilling factor の診断 TiIによる黒点暗部のベクトル磁場	12	122
6563	偏光測定は無理、彩層・プロミネンス構造、速度場	119	>2000

観測プラニング事始

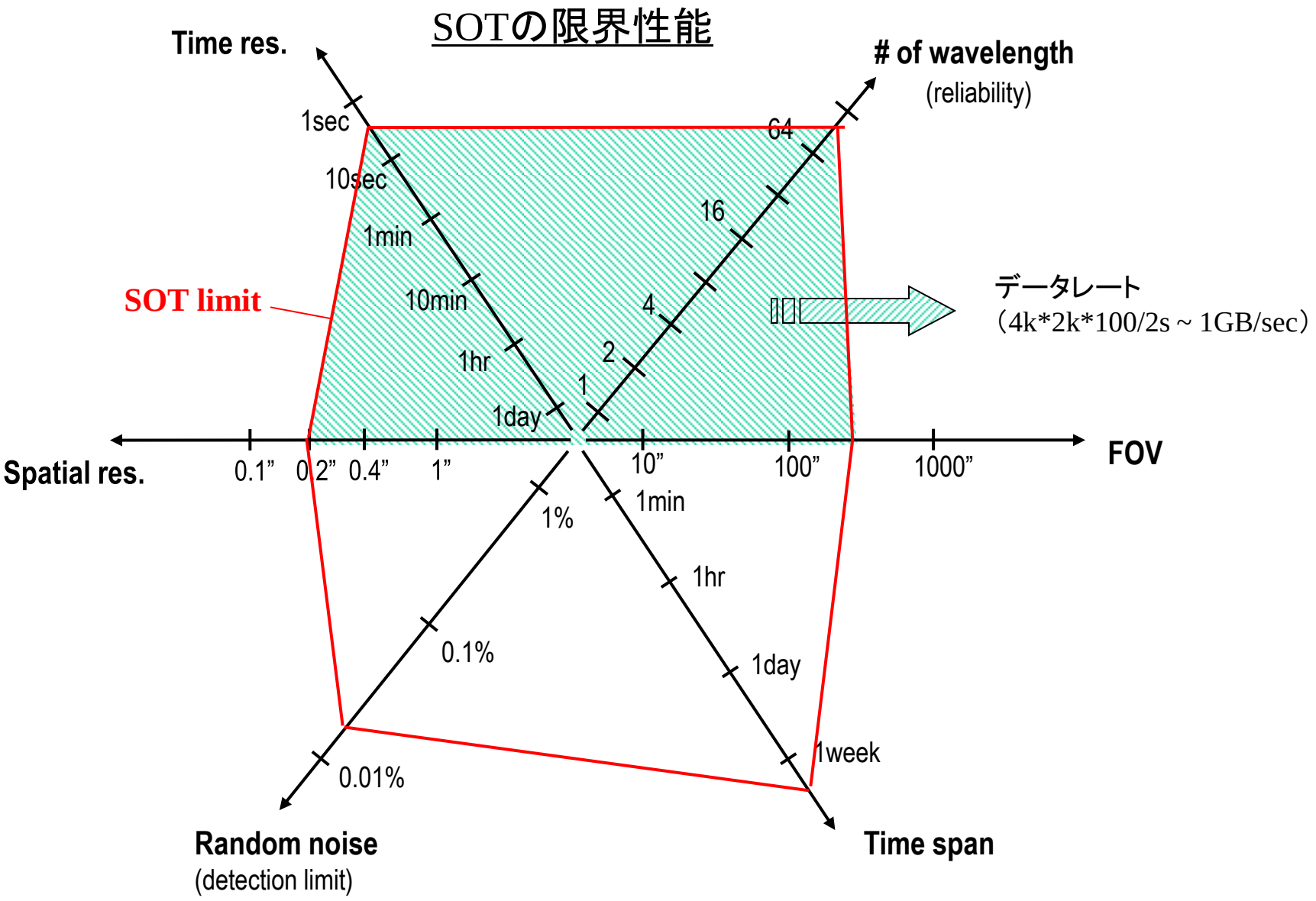
SOTの限界性能
Time res.
1sec
10sec
1min
10min
1hr
1day
# of wavelength
(reliability)
64
16
4
2
1
SOT limit
データレート
（4k*2k*100/2s ~ 1GB/sec）
Spatial res.
0.1”
0.2”
0.4”
1”
10”
100”
1000”
FOV
1%
0.1%
0.01%
1min
1hr
1day
1week
Random noise
(detection limit)
Time span

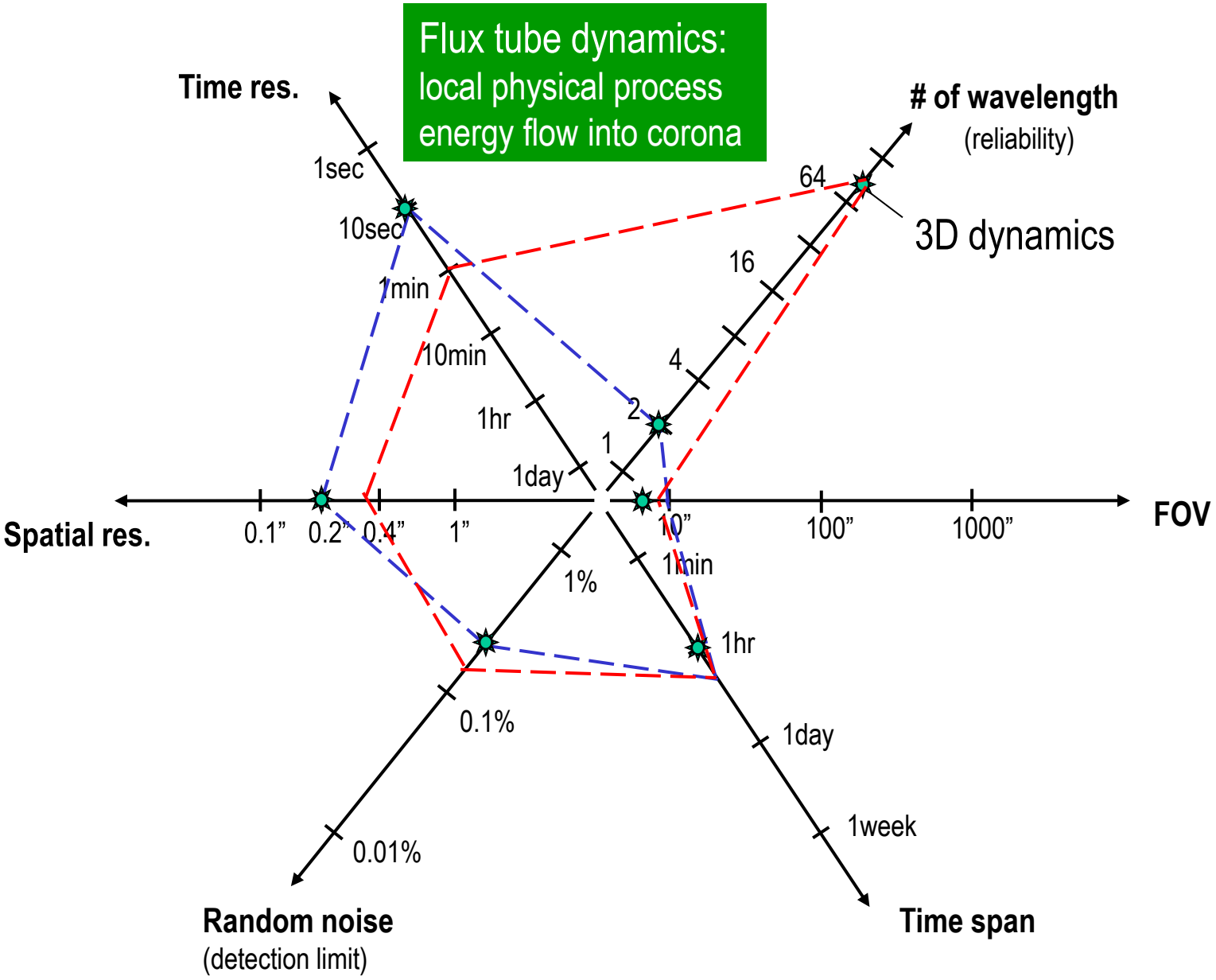
Flux tube dynamics:
local physical process
energy flow into corona
Time res.
1sec
10sec
1min
10min
1hr
1day
# of wavelength
(reliability)
64
16
4
2
1
3D dynamics
Spatial res.
0.1”
0.2”
0.4”
1”
10”
100”
1000”
FOV
1%
0.1%
0.01%
Random noise
(detection limit)
1min
1hr
1day
1week
Time span

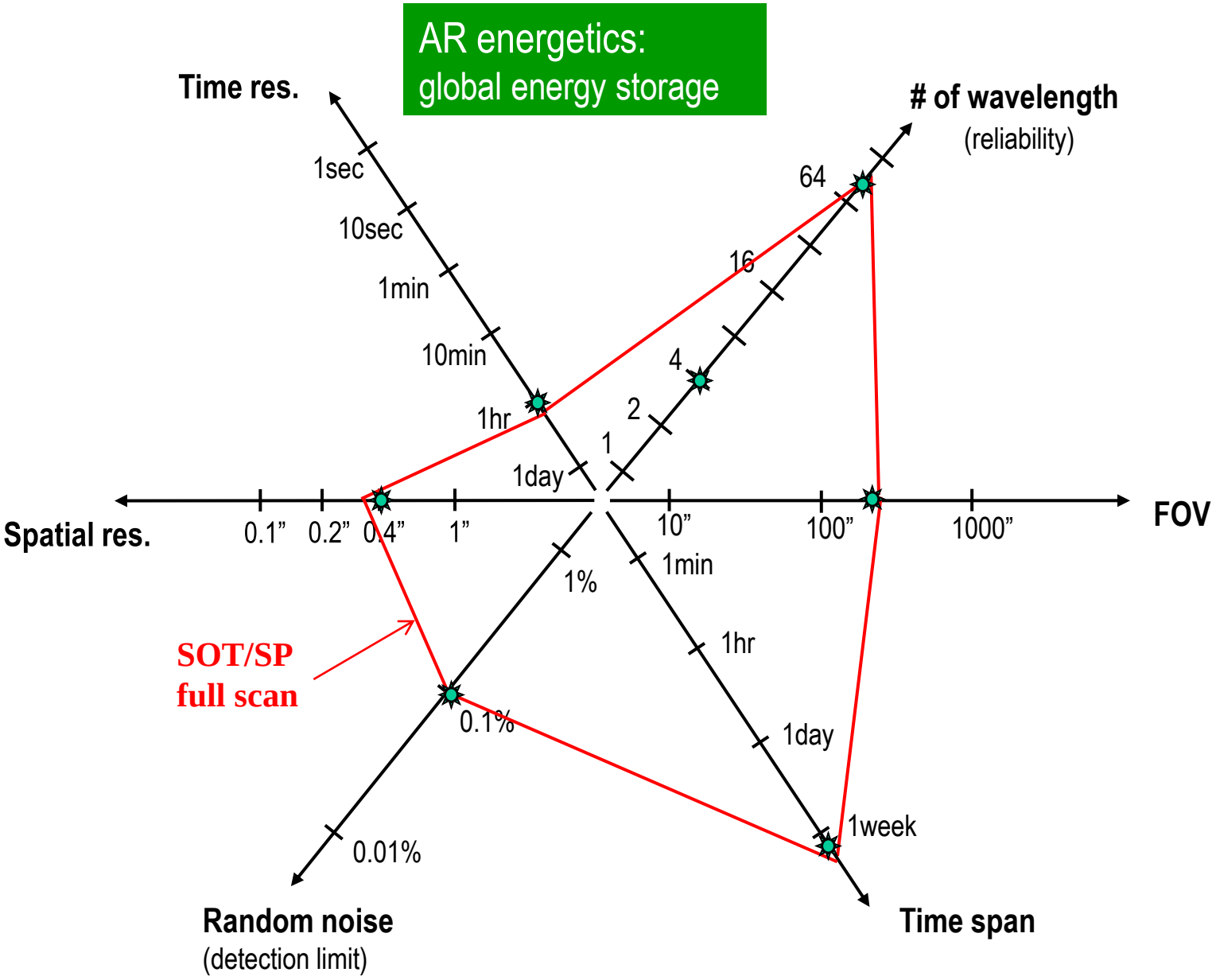
AR energetics:
global energy storage
Time res.
1sec
10sec
1min
10min
1hr
1day
# of wavelength
(reliability)
64
16
4
2
1
Spatial res.
0.1”
0.2”
0.4”
1”
10”
100”
1000”
FOV
SOT/SP
full scan
1%
0.1%
0.01%
Random noise
(detection limit)
1min
1hr
1day
1week
Time span

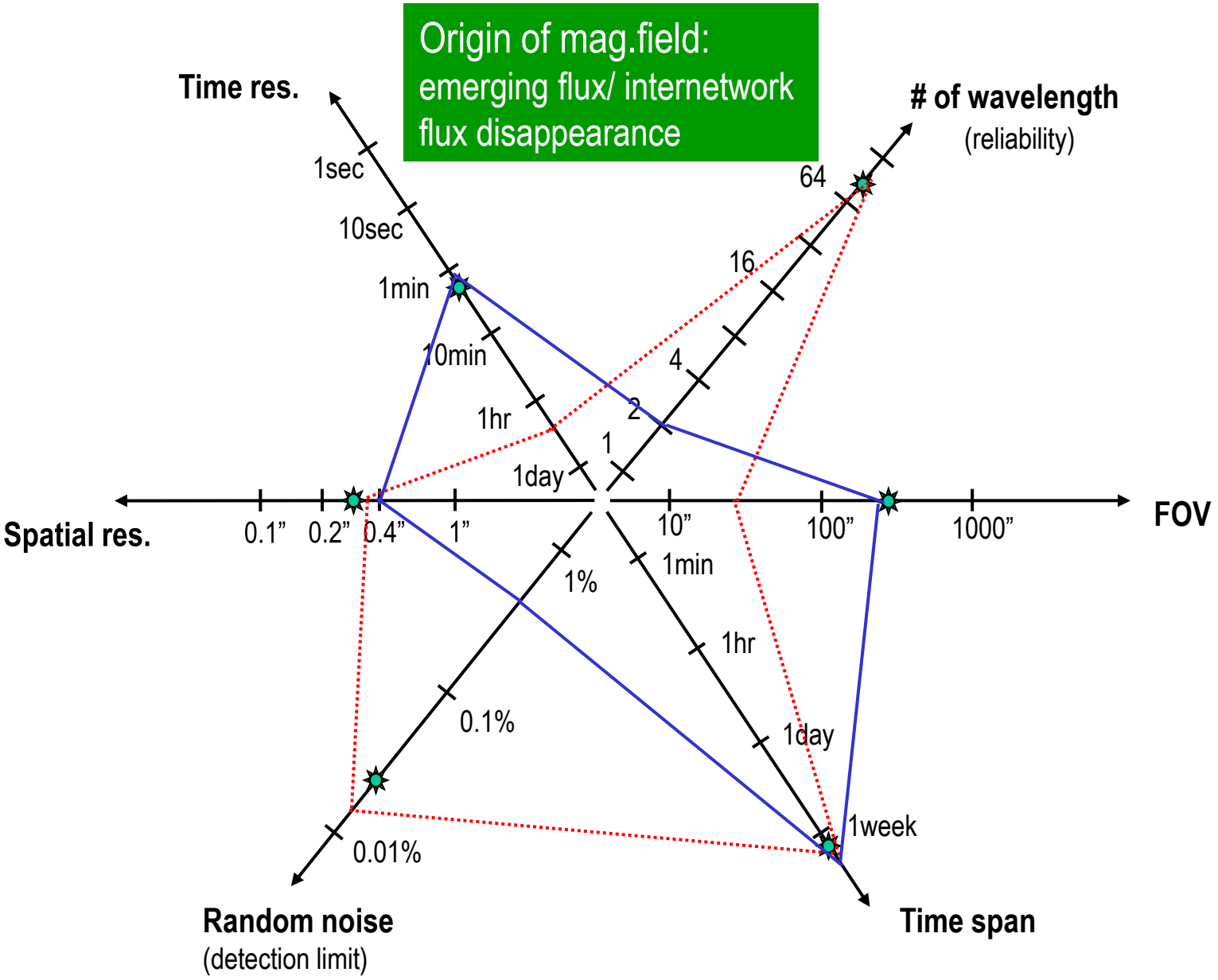
Origin of mag.field:
emerging flux/ internetwork
flux disappearance
Time res.
1sec
10sec
1min
10min
1hr
1day
# of wavelength
(reliability)
64
16
4
2
1
Spatial res.
0.1”
0.2”
0.4”
1”
10”
100”
1000”
FOV
1%
0.1%
0.01%
Random noise
(detection limit)
1min
1hr
1day
1week
Time span